

1 Fine-scale spatial genetic structure in a locally abundant native bunchgrass (*Achnatherum* 2 *thurberianum*) including distinct lineages revealed within seed transfer zones

3 Carolina Osuna-Mascaró¹, Alison C. Agneray^{2,3}, Lanie M. Galland³, Elizabeth A. Leger^{1,3}, and
4 Thomas L. Parchman^{1,3}

5

⁶ ¹Department of Biology, University of Nevada, Reno, NV 89557, USA

⁷ ²US Department of the Interior Bureau of Land Management, Reno, NV 89502, USA

⁸ ³Ecology, Evolution, and Conservation Biology Program, University of Nevada, Reno, NV 89557,
⁹ USA

¹⁰ Corresponding author: Carolina Osuna-Mascaró

11 1664 N. Virginia Street

12 Department of Biology, 100

13 University of Nevada, Reno

14 Reno, NV 89557, USA

15 cosuna@unr.edu

16 Running title: Landscape genetics of Thurber's needlegrass

17 **Key words:** ddRADseq, genetic diversity, local adaptation, restoration genetics, spatial genetic
18 structure, *Achnatherum thurberianum*

19

20 **Abstract**

21 Analyses of the factors shaping spatial genetic structure in widespread plant species are important
22 for understanding evolutionary history and local adaptation and have applied significance for
23 guiding conservation and restoration decisions. Thurber's needlegrass (*Achnatherum*
24 *thurberianum*) is a widespread, locally abundant grass that inhabits heterogeneous arid
25 environments of western North America and is of restoration significance. It is a common
26 component of shrubland steppe communities in the Great Basin Desert, where drought, fire, and
27 invasive grasses have degraded natural communities. Using a reduced representation sequencing
28 approach, we generated SNP data at 5,677 loci across 246 individuals from 17 *A. thurberianum*
29 populations spanning five previously delineated seed zones from the western Great Basin.
30 Analyses revealed pronounced population genetic structure, with individuals forming consistent
31 geographical clusters across a variety of population genetic analyses and spatial scales. Low levels
32 of genetic diversity within populations, as well as high population estimates of linkage
33 disequilibrium and inbreeding, were consistent with self-fertilization as a contributor to population
34 differentiation. Moreover, variance partitioning and partial RDA indicated local adaptation to the
35 environment as an additional factor influencing the spatial distribution of genetic variation. The
36 environmental variables driving these results were similar to those implicated in recent
37 genecological work which inferred local adaptation in order to delineate seed zones. However, our
38 analyses also reveal a complex evolutionary history of *A. thurberianum* in the Great Basin, where
39 previously delineated seed zones contain distantly related populations. Overall, our results indicate
40 that numerous factors shape genetic variation in *A. thurberianum* and that evolutionary history,
41 along with differentiation across distinct geographic and environmental scales, should be
42 considered for conservation and restoration plans.

43

44 **Introduction**

45 Identifying the factors that drive patterns of genetic variation among plant populations is important
46 for understanding ecological and evolutionary processes and has applied significance for
47 conservation and ecological restoration (Sork et al., 1999; Hedrick, 2005; Holderegger and Wagner
48 2008; Sommer et al., 2013). The spatial distribution of genetic variation reflects evolutionary
49 processes, including drift, migration, and selection, which shape the standing variation and the
50 evolutionary potential of populations. Therefore, quantifying spatial genetic structure and the
51 factors shaping it can help assess the degree of population connectivity, the scale of and potential
52 for local adaptation to environmental variation, and, consequently, the persistence of plant
53 populations faced with environmental change (Bauert et al., 1998; Booy et al., 2000; Manel et al.,
54 2003). Such analyses can also be used to guide conservation and restoration decisions using
55 biologically meaningful information (Ottewell et al., 2016; Carvalho et al., 2021). During the last
56 decade, high throughput sequencing approaches have substantially improved our ability to
57 quantify spatial genetic structure and infer its causes across populations of ecologically significant
58 non-model organisms (Andrews et al., 2016; Breed et al., 2019; Hohenlohe et al., 2021).

59 For plant species with large distributions spanning heterogeneous environments, spatial
60 genetic structure can be shaped by numerous factors, including geological, historical, and
61 environmental factors, as well as life-history variation (Holderegger et al., 2010). Across large
62 geographic scales, genetic differentiation among populations can be expected as gene flow decays
63 with increasing geographic distance and across geological barriers, commonly resulting in
64 isolation by distance (Wright, 1943; Gavrilets et al., 2000; Hoskin et al., 2005). However,
65 environmental and ecological factors may also play a role in shaping spatial genetic structure
66 (Alvarez et al., 2009; Storfer et al., 2010; Paz et al., 2015; Mosca et al., 2018). Environmental

67 variation can directly influence genetic differentiation by causing local adaptation and indirectly
68 by generating Isolation by Environment (IBE; Shafer and Wolf, 2013; Wang and Bradburd, 2014),
69 where gene flow is reduced across environmental gradients or selection against migrants occurs
70 (Kawecki and Ebert, 2004). Thus, strong population genetic differentiation can occur across
71 regions experiencing different ecological and environmental conditions (Ortego et al., 2012; Orsini
72 et al., 2013; Wang et al., 2013; Wang and Bradburd, 2014).

73 Mating system also influences patterns of population genetic structure in plants (Williams
74 et al., 2001; Duminil et al., 2007; Gamba and Muchhal, 2020), due to variation in the frequency
75 with which offspring are produced asexually, through self-fertilization, or via sexual outcrossing
76 (Holsinger, 2000). Compared to outcrossers, asexual and selfing plants often have reduced levels
77 of within-population genetic diversity. In particular, selfing plants often exhibit low population
78 genetic variation and high inbreeding which can lead to relatively pronounced patterns of
79 population differentiation (Hamrick and Godt, 1996; Volis et al., 2010; Wagner et al., 2012; Huang
80 et al., 2021). Thus, selfing plants may show stronger patterns of population structure at a local
81 scale and lower genetic diversity than outcrossing plants with higher genetic diversity and non-
82 structured populations. Mating system could thus impact another decision increasingly common
83 in restoration, which is whether to combine collections from multiple populations, either to
84 deliberately increase diversity or as a practical decision when there are simply not enough seeds
85 available from one population (St. Clair et al., 2020). While there is concern about the potential
86 for outbreeding depression when combining populations of outbreeding species (Templeton, 1986;
87 Hufford et al., 2012), these concerns could be reduced for highly inbreeding species.

88 In complex environments, isolation and convergent evolution can result in similar but
89 independently derived phenotypes in populations with very different evolutionary histories (St.

90 Clair et al., 2013; Massatti et al., 2018). While common in natural systems, these patterns may
91 confound restoration efforts, leading to situations where practitioners may be choosing between
92 seed sources that either possess phenotypes that are likely to be adaptive in a given site but are
93 distantly related to plants that used to occur there, or are more closely related to former inhabitants,
94 maintaining historical patterns of gene flow, but with sub-optimal phenotypes that may not survive
95 as well in restoration sites (Leger et al., 2021). Historically, evolutionary history has been
96 commonly considered in conservation planning for rare species (Verdú et al., 2012), while an
97 emphasis on adaptive phenotypes has been the focus for delineating seed transfer zones for
98 restoration of widely-distributed species (Baughman et al., 2019; Pedlar et al., 2021). However,
99 due to advances in DNA sequencing technology, it has recently become possible to consider
100 evolutionary history as well as both genomic and phenotypic evidence for local adaptation for
101 widely distributed species (Massatti et al., 2018; Breed et al., 2019). Here we consider how
102 evolutionary history and environmental variation shape landscape genetic structure in a
103 widespread grass species of restoration significance in the Great Basin Desert, for which seed
104 transfer zones have been previously inferred based on phenotypic evidence for local adaptation
105 (Johnson et al. 2017).

106 The Great Basin is the most extensive cold desert in North America, with an area of about
107 540,000 km², that harbors significant environmental heterogeneity and biological diversity,
108 including high levels of genetic diversity and local adaptation across extensive environmental
109 gradients created by the complex, repeated basin and range topography (West, 1983; Pilliod et al.,
110 2017; Baughman et al., 2019; Faske et al., 2021). However, in recent decades, the combined effects
111 of altered fire regimes, invasive annual grasses, and human land use have led to widespread
112 degradation and fragmentation of habitats in the Great Basin (Balch et al., 2013; Pilliod et al.,

113 2013). In particular, cheatgrass (*Bromus tectorum*) and other non-native annual species have
114 transformed native shrublands into invasive-dominated grasslands (Knapp, 1996; Parkinson et al.,
115 2013; Nagy et al., 2021). These factors, along with climate change, are contributing to native plant
116 species declines, especially native grasses, many of which are decreasing in abundance (Chambers
117 and Wisdom, 2009; Svejcar et al., 2017). Overall, restoration efforts are increasing in response to
118 global initiatives (Dudley et al., 2020; Stange et al., 2021), especially in drylands such as the Great
119 Basin (Pilliod et al., 2017; Shackelford et al., 2021). Despite the widely recognized importance of
120 considering spatial genetic structure and local adaptation for restoration planning (Knapp and Rice,
121 1994; Hufford and Mazer, 2003; McKay et al., 2005; Breed et al., 2019), and the growing number
122 of plants in this region with phenotype-based seed transfer zones (TRM Seed Zone Applications:
123 <https://www.fs.fed.us/wwetac/threat-map/TRMSeedZoneMapper.php>), we lack population
124 genomic perspectives for most Great Basin native plants of restoration significance (but see
125 Massatti et al., 2018).

126 Among the Great Basin grass species of restoration interest is Thurber's needlegrass,
127 *Achnatherum thurberianum* (Piper) Barkworth, a widespread perennial bunchgrass species and an
128 essential component of many sagebrush communities (Johnson et al., 2017). *Achnatherum*
129 (Poaceae, subfamily Pooideae, tribe Stipeae) consists of large perennial grasses that grow in
130 temperate grassland and savannah habitats (Soreng et al., 2015; Soreng et al., 2017), many of
131 which are thought to self-fertilize (Jones and Nielson, 1989; Durka et al., 2013; Kraehmer, 2019).
132 Genetic boundaries of *Achnatherum* are controversial (Jacobs et al., 2007; Cialdella et al., 2010;
133 Romaschenko et al., 2010, 2012; Peterson and Romaschenko, 2019), and accordingly, the
134 taxonomy of the genus has been reviewed several times (Hamasha et al., 2012). In particular, *A.*
135 *thurberianum* has been previously classified as *Stipa thurberiana* (Piper), (Circ. Div. Agrostol.

136 U.S.D.A., 1900), *A. thurberianum* (Piper), (Barkworth, 1993), and the more recent although not
137 yet widely in use *Eriocoma thurberiana* (Piper) (Peterson and Romaschenko, 2019; see the
138 Missouri Botanical Garden's taxonomic database; <http://www.tropicos.org>). Studies on related
139 species in Eurasia (from the tribe Stipeae) based on traditional molecular markers indicated
140 pronounced population differentiation and low diversity consistent with a selfing mating system
141 and demographic processes shaping population differentiation at small spatial scales (Wagner et
142 al., 2012; Durka et al., 2013). Other studies on Eurasian species have indicated the potential for
143 climate to shape local adaptation and population genetic structure (Hamasha et al., 2013; Gao et
144 al., 2018; Schubert et al., 2019). Recent genecological work on *A. thurberianum* phenotypes across
145 the Great Basin illustrated local adaptation in response to temperature and precipitation variation,
146 which led to the formation of seed transfer zones for this species (Johnson et al., 2017).
147 Specifically, in that study, populations from warmer and drier regions generally exhibited earlier
148 flowering time and narrower leaves than those from cooler wetter regions (Johnson et al., 2017).
149 However, we currently lack a baseline perspective on the spatial distribution of genetic variation
150 for *A. thurberianum* in the Great Basin region, which is important because a complex evolutionary
151 history could have unintended consequences for seed sourcing if transfer zones are delineated
152 based on only climate, proximity, or phenotypic evidence for local adaptation (Massatti et al.,
153 2018). Analyses of evolutionary history and how landscape genetic variation is shaped by
154 environmental, geographic, and life history variation stand to improve understanding of the
155 biology of this widespread species and provide a critical context for understanding its evolution
156 and restoration potential, including the application of phenotype-based seed transfer zones
157 (Johnson et al., 2017).

158 Here, we used reduced representation sequencing (ddRADseq) to characterize spatial
159 genetic variation across 17 *A. thurberianum* populations distributed across the southwestern Great
160 Basin, in an area representing five of the twelve seed zones proposed by Johnson et al. (2017). We
161 examined phylogeographic patterns and spatial genetic structure across populations and
162 considered how geographical and environmental factors influenced them. We also quantified
163 levels of genetic diversity, linkage disequilibrium, and inbreeding coefficients within populations
164 to evaluate the extent to which mating system might influence standing variation and fine-scale
165 differentiation across the sampled populations and asked to what degree existing seed zones
166 reflected evolutionary history. We expected to see pronounced regional and fine-scale spatial
167 genetic structure, influenced by both mating system and local adaptation to environmental
168 variation in this widespread grass. Further, we expected that we might find evidence of multiple
169 lineages represented within seed zones, given the complexity of the basin and range topography
170 and the potential for convergent evolution during the process of local adaptation.

171 **Material and methods**

172 Plant material

173 We collected leaf material from 17 localities in the western Great Basin during the Fall of 2017
174 from a range of 20 to 39 plants per location (Figures 1a, 2a; Table 1). We sampled these locations
175 because they hosted multiple native species that could potentially serve as restoration seed sources
176 for this region; collections of other species from these locations are being used for additional
177 restoration genetic studies (e.g., Faske et al., 2021; Agneray et al., 2022). In addition, these
178 localities spanned five seed zones proposed by Johnson et al., (2017). Means for representative
179 environmental variables for each population were obtained as described below and can be found
180 in Suppl. Table 1. Because of the complex topography in this region, note that proximate

181 populations are not necessarily within the same seed zone (Figure 1a). A total of 246 individuals,
182 from a range of 12 to 18 plants per location, were included in analyses after DNA extraction and
183 quality screening (see below).

184 Library preparation, sequencing, and variant calling

185 DNA was extracted from dried tissue using Qiagen DNeasy Plant Mini Kits and quantified with a
186 Qiagen QIAxpert microfluidic analyzer (Qiagen Inc., Valencia, CA, USA). We constructed
187 reduced-representation libraries for Illumina sequencing using a ddRADseq method (Parchman et
188 al., 2012; Peterson et al., 2012). The genomic DNA was digested with two restriction enzymes,
189 *EcoRI* and *MseI*, and custom oligos with Illumina base adaptors and unique barcodes were ligated
190 to the digested fragments (ranging from eight to 10 base pairs in length). Ligated fragments were
191 amplified by PCR using a high-fidelity proofreading polymerase (iProof High-Fidelity DNA
192 Polymerase, BioRad Inc., Hercules, CA, USA) and subsequently pooled into a single library.
193 Libraries were size selected for fragments between 350 and 450 bp in length with the Pippin Prep
194 System (Sage Sciences, Beverly, MA) at the University of Texas Genome Sequencing and
195 Analysis Facility (UTGSAF). Sequence data were generated for the full set of individuals using a
196 partial lane of sequencing on the Illumina NovaSeq platform at the UTGSAF.

197 We used the tapioca pipeline (<https://github.com/ncgr/tapioca>) and a known contaminant
198 sequence database to identify and discard Illumina primer/adapter sequences and potential
199 biological sequence contaminants (e.g., PhiX, *E. coli*). We then demultiplexed the reads using a
200 custom Perl script that corrects one or two base sequencing errors in barcoded regions, parse reads
201 according to their associated barcode sequence, and trims restriction site-associated bases.
202 Trimmed fastq files for each individual are available at SRA ([https:](https://)).

203 Filtered reads were clustered for variant identification and filtering with the software
204 `Stacks v 1.46` (Catchen et al., 2013). We followed a *de novo* assembly approach, using the
205 "denovo_map.pl" module, which allows genotype inference by identifying SNP loci without a
206 reference genome. The parameters were set as follows: the minimum number of identical reads
207 required to call an allele was set to 3 ($m = 3$), the maximum number of mismatches between loci
208 for individuals was set to 2 ($M = 2$), and the maximum number of mismatches among loci when
209 comparing across individuals was set to 2 ($n = 2$). These parameters were selected through an
210 optimization process following recommendations from Mastretta-Yanes et al., (2015) and Paris et
211 al., (2017). In brief, we set the optimal m among values ranging 2 to 7 (for M and $n = 2$) and the
212 optimal M value among values ranging from 2 to 6 for the m optimal value (for $n = M$). Then, we
213 used the "populations" module in `Stacks` (Catchen et al., 2011, 2013; Rochette et al., 2019) to
214 extract loci that were present in at least 80% of the individuals ($--r = 0.80$) and with a maximum
215 observed heterozygosity of 0.65 ($--max_obs_het = 0.65$) and to generate and export the SNP data
216 in vcf format for further analyses. We used `vcftools v 4.2` (Danecek et al., 2011) to estimate
217 the allele frequency, the mean depth per individual, the mean depth per site, and the proportion of
218 missing data per site of the vcf outputs. We explored these statistics in R in order to decide the
219 optimal m , M , and n parameters. Additionally, we filtered the obtained pool of loci using `vcftools`
220 `v 4.2`. We allowed a maximum missing data of 20 % ($--max-missing 0.8$), a minimum minor
221 allele frequency of 0.03 ($--maf 0.03$) and specified a thin value of 5 ($--thin 5$), which allows that
222 no two sites are within the specified distance from one another. Also, we only included sites with
223 quality scores above 10 ($--minQ 10$).

224 Patterns of population genetic diversity and differentiation

225 Genetic diversity estimates were calculated in R using the package `hierfstat v 0.5-7` (Goudet,
226 2005). We used the "basic.stats" function to estimate mean observed heterozygosity (H_o), mean
227 expected heterozygosity (H_e), and individual inbreeding coefficients (F_{IS}) within each population.
228 Pairwise Nei's F_{ST} (Nei, 1987) and pairwise genetic distances (Nei's D) were estimated for all
229 pairs of populations with the "genet.dist" function. The confidence intervals over F_{IS} and F_{ST}
230 values were estimated using 1000 bootstraps with the "boot.ppfis" function. Additionally, we
231 estimated nucleotide diversity (π) and Tajima's D for each population, using `vcftools v 4.2`.

232 We further quantified genetic structure within and among populations with an analysis of
233 molecular variance (AMOVA) using the R package `poppr v 2.9.2` (Kamvar et al., 2014). We
234 tested whether most genetic variance was observed among individuals within populations (i.e., no
235 population structure) or between populations (i.e., population structure). The significance of
236 AMOVA results was tested with the function "randtest" from the R package `adegenet v 1.3-1`
237 (Jombart, 2008) using 999 simulations. A linkage disequilibrium (LD) analysis was conducted
238 based on the index of association (I_A ; Brown et al., 1980) and the standardized index of association
239 (r_d^-) over all the loci to infer the mode of reproduction within populations. Linkage disequilibrium
240 is expected to be more pronounced in populations engaging in selfing or asexual reproduction in
241 comparison to those mainly reproducing sexually. We used the package `poppr v 2.9.2` (Kamvar
242 et al., 2014) and performed the analysis using 999 permutations. To distinguish between selfing
243 and asexual reproduction as processes leading to low genetic diversity, we estimated relatedness
244 among individuals using `vcftools v 4.2` based on the Manichaikul et al., (2010) approach (--
245 relatedness2). This method gives information about the relationship of any pair of individuals by
246 assessing their kinship coefficient, which ranges from 0 (no relationship) to 0.50 (self). Individuals

247 were plotted against one another using the "heatmap" function from the R package `stats` v 3.3.1
248 (Team, R. C., 2013).

249 Spatial genetic structure

250 We tested whether populations exhibited isolation by distance (IBD; Wright, 1943) and/or
251 isolation by environment (IBE; Wang & Bradburd, 2014), comparing the pairwise matrices of
252 genetic distances (Nei's D; see above) with geographic and environmental distances (see
253 environmental data details below) through Mantel tests. We used the "mantel" function from the
254 R package `vegan` v 2.5-7 (Oksanen et al., 2013), with Spearman correlation and 9999
255 permutations. We estimated the geographic distances among populations as haversine distances
256 using the "distm" function of the `geosphere` v 1.5-14 R package (Hijmans et al., 2017).

257 Spatial genetic variation was further assessed using model-free and model-based inference
258 of genetic variation among individuals. First, we inferred population structure and individual
259 ancestries without *a priori* information on sample origin using `ADMIXTURE` v 1.3.0 (Alexander
260 and Lange, 2011). We used `PLINK` v 1.07 (Purcell et al., 2007) to convert the vcf file into unlinked
261 SNPs (i.e., LD-pruned SNPs) and then ran `ADMIXTURE` with K values ranging from 2 to 10. The
262 optimal value of K was estimated by evaluating cross-validation errors. Patterns of genetic
263 variation were further summarized by principal component analyses (PCA; Patterson et al., 2006)
264 using the "prcomp" function from the R package `stats` v 3.3.1 (Team, R. C., 2013). For each
265 ancestral population (k) we indicated the corresponding seed zone of Johnson et al. (2017). We
266 also performed uniform manifold approximation and projection analyses (UMAP; Leland et al.,
267 2018; McInnes et al., 2018) using the "umap" function from the R package `umap` v 0.2.7.0
268 (Konopka, 2020). UMAP has recently been shown to excel at detecting and conveying fine-scale
269 spatial genetic structure of populations (Diaz-Papkovich et al., 2019; Diaz-Papkovich et al., 2021).

270 We ran UMAP with the minimum distance between points in low-dimensional space (MD) ranging
271 from 0.1 to 0.99 and the number of approximate nearest neighbors used to construct the initial
272 high-dimensional graph (NN) ranging from two to 16. Based on an assessment of clustering results
273 across this range of parameter space (Suppl. Figures 2 a-h), we present results here with min_dist
274 = 0.25 and n_neighbors = 16.

275 We conducted two analyses to visualize variation in differentiation and effective migration
276 across the sampled populations. Both analyses essentially quantify the extent to which
277 differentiation among populations departs from the expectation of isolation by distance. First, we
278 visualized effective migration rates using EEMS (Estimated Effective Migration Surfaces; Petkova
279 et al., 2016). This analysis assigns individuals to the nearest deme, and by using a stepping-stone
280 model, estimates effective migration rates between demes. A genetic dissimilarity matrix was
281 calculated using the bundled bed2diffs script (Petkova et al., 2016). The habitat polygon was
282 obtained manually to include the sampling localities of all the populations, using Google Maps
283 API v 3 Tool (<http://www.birdtheme.org/useful/v3tool.html>). We chose a deme size of 300
284 (nDemes parameter) and performed three independent analyses using runeems_snps script, with a
285 burn-in of 100,000,000 (numBurnIter parameter), MCMC length of 200,000,000 (numMCMCIter
286 parameter), and the number of iterations to thin between two writing steps of 999,999
287 (numThinIter parameter). We combined the results of the three independent runs and plotted the
288 results corresponding to the surfaces of effective diversity (q) and effective migration rates (m)
289 using the R package rEEMSplots v 0.0.1 (Petkova et al., 2016).

290 As an additional method to visualize differentiation and effective migration across
291 populations, we employed unbundled principal components (unPC) as a complementary method
292 to EEMS, to reveal potential long-distance migration using the unPC v 0.1.0 R package (House

293 and Hahn, 2018). UnPC uses principal components in combination with geographic coordinates
294 of samples to create visualizations of genetic differentiation across the landscape. It first calculates
295 the Euclidean distance between PCA coordinates for each pair of populations and then estimates
296 the pairwise geographic distance between populations. The ratio of the genetic distance to the
297 geographic distance for each pair of populations is the unPC value for each pair.

298 Finally, we analyzed and visualized population structure using a phylogenomic approach.
299 First, we converted the vcf file to fasta format using `vcf2phylip v 2.0` (Ortiz, 2019). We trimmed
300 the fasta alignment to exclude unreliably aligned positions with `trimAl v 1.2` using the
301 "gappyout" method (Capella-Gutiérrez et al., 2009). Then, we ran `IQ-TREE v 1.6.10` (Nguyen et
302 al., 2015) using the "Model Finder Plus" parameter (-m MFP) to determine the best substitution
303 model (choosing the model that minimizes the BIC score), the ascertainment bias correction
304 method (ASC; Lewis, 2001), and the ultrafast bootstrap option with 1000 bootstrap replicates (-bb
305 1000). We visualized the obtained tree in `Figtree v 1.4.4` (Rambaut, 2018), and indicated the
306 appropriate seed zone for each sampled individual. We then plotted the tree linked with the
307 population's geographical coordinates after simplifying the tree to retain one sample tip per
308 population using the `drop.tip` function in the R `ape` package v 5.5 (Paradis et al., 2004). We
309 used the "phylo.to.map" function in the R package `phytools v 0.7-80` to plot a map (Revell,
310 2014), using the dropped tree and the geographical coordinates and choosing the "state" database,
311 again indicating seed zone for each population. To quantify the extent to which seed zones reflect
312 evolutionary history, we tested for phylogenetic signal by estimating Pagel's λ (Pagel, 1999) for
313 the distribution of seed zones across sampled populations. We used the "fitDiscrete" function from
314 the R package `geiger v 2.0.7` (Harmon et al., 2015). To test the significance of our results, we

315 estimated the log-likelihood if $\lambda = 0$ and if $\lambda = 1$ using the function “rescale” and did a likelihood
316 ratio test.

317 Influence of environmental variation on spatial genetic variation

318 We conducted genetic-environment association (GEA) analyses using partial redundancy analysis
319 (pRDA) to identify environmental variables that covary with genetic differentiation among
320 populations. Climate environmental variables for each site were obtained from the PRISM
321 database (<https://prism.nacse.org>) using the "get_prism_normals" function from the R prims
322 library (Hart et al., 2015), with a data range from 1981 to 2010 with an 800 m x 800 m resolution.
323 Following Faske et al., (2021), we converted monthly normals to estimates of potential
324 evapotranspiration, actual evapotranspiration, soil water balance, and climatic water deficit, which
325 have been shown to effectively predict aspects of spatial and distributional variation across plant
326 communities (Barga et al., 2018). Elevation data was acquired from the R library elevatr v
327 0.2.0 (Hollister and Shah, 2017). We also included several climatic variables that predicted
328 genecological variation and were used for seed zone delineation in a previous study (Johnson et
329 al. 2017; see Suppl. Tables 2a, b for details). Before any analyses, we examined multicollinearity
330 among the pool of variables using the “pairs.panels” function from the psych v 2.1.9 R package
331 (Revelle, 2015), based on Pearson's $|r| \leq 0.60$, to select the most orthogonal subset of variables
332 possible. We removed all the environmental variables that were highly correlated with other
333 variables, thus reducing the data set from 46 to 8 environmental variables (Table 2). Then, we
334 applied partial redundancy analysis variance partitioning to decompose the contribution of climate,
335 population structure, and geography in explaining genetic variation. We used three sets of
336 variables: 1) climate environmental variables (Table 2); 2) two proxies of genetic structure
337 (population scores along the two previously estimated PC axes); and 3) each population's

338 coordinates (longitude and latitude). As a response variable, we used the individual-based
339 genotypes (coded as the count of one allele, i.e., 0/1/2). We used the "rda" function from the vegan
340 v 2.5-7 R package (Oksanen et al., 2013) for pRDA. Following Capblancq and Forester (2021),
341 we first tested the significance of the full RDA model (with all the variables included).
342 Subsequently, explanatory variables were added one by one, using the "ordiR2step" function of
343 the vegan v 2.5-7 R package, with the following stopping criteria: variable significance of $p <$
344 0.01, 1000 permutations, and the adjusted R2 of the global model. Then, we performed three
345 different pRDA models: first, a model accounting for environmental variables only (conditioning
346 the model by geography and population structure); second, a model accounting for population
347 structure (conditioning the model by geography and environmental variables); and third, a model
348 accounting for geography (conditioning the model by population structure and environmental
349 variables). We then compared the amount of variance explained by each pRDA to the variance of
350 the full model (including all explanatory variables) to estimate the independent contribution of
351 each set of variables together with any confounding effects induced by collinearity.

352 Given the results from the above analyses, we conducted pRDA on the genotypic and
353 environmental data to infer the influence of specific environmental variables on spatial genetic
354 structure and detect the genetic signal of local adaptation and its environmental causes. We used a
355 partial RDA (pRDA) conditioning by population structure (PC1 and PC2) and geography (latitude
356 and longitude) to assess whether the degree of adaptive genetic variation among individuals is
357 explained by a particular set of environmental variables. The significance of models and RDA
358 axes, and the proportion of variation explained by each environmental variable were tested with
359 an analysis of variance (ANOVA) and permutation ($n = 999$), using the "anova.cca" function of
360 the vegan v 2.5-7 R package. Also, we used RDA to identify outlier loci potentially under

361 selection using loadings of SNPs from the first three constrained ordination axes. We used
362 stringent outliers filtering of 3.5 standard deviations ($p < 0.0005$) (Forester et al., 2018). Then, we
363 checked for duplicate candidate loci associated with more than one RDA axis and used Pearson's
364 correlation (r) to identify the strongest predictor.

365 Results

366 Patterns of genetic diversity and differentiation

367 We identified a total of 5,677 SNPs in a subset of 246 individuals that were retained after filtering
368 with mean coverage depth per individual of 21.83. Population genetic statistics were obtained for
369 each population (Table 1). Observed heterozygosity (H_o) values were lower than the expected (H_e)
370 in all the cases, indicating low heterozygosity in all the populations studied. As follows, inbreeding
371 coefficient (F_{IS}) values were positive for all populations, indicating reduced diversity that is
372 consistent with self-pollination. F_{IS} values were variable across populations but were significantly
373 positive for all populations except DH, EW, SC, SS, and VM, based on bootstrap coefficient
374 intervals. Nucleotide diversity (π) estimates were low, congruent with previous results. Moreover,
375 all populations had positive values of Tajima's D consistent with population size contraction. The
376 index of association (I_A) and the standardized index of association (r_d^-) were different from zero
377 and significant in all cases ($p < 0.001$), indicating elevated levels of linkage disequilibrium
378 consistent with selfing influencing variation within populations. Lastly, 98.58 % of the pairwise
379 combinations among individuals had mean relatedness coefficients of 0, and 1% had a mean
380 relatedness coefficient of 0.33, ranging from 0.005 to 0.47 (considering the 1 % left from
381 comparisons among same individuals) indicating that populations are diverse and do not consist
382 of apomicts (see Suppl. Table 3 and Suppl. Figure 1).

383 Spatial genetic structure

384 AMOVA analyses indicated that 79.66 % ($p < 0.01$) of the observed genetic variance was
385 explained by variation between populations, consistent with strong population differentiation, with
386 the remaining 20.33 % ($p < 0.01$) reflecting variation among individuals within populations (Table
387 3). The results of the Mantel test indicated a positive association between geographic distance and
388 genetic distance (IBD: Mantel statistic r : 0.257, p : 0.026; Figure 2a) and between environmental
389 and geographic distances (Mantel r : 0.238, p : 0.025; Figure 2c). No significant association was
390 found between environmental and genetic distances (Mantel statistic r : -0.001, p : 0.437; Figure
391 2b).

392 Population pairwise F_{ST} values were significant in all pairwise comparisons (mean: 0.18,
393 range: 0.02 – 0.31), even for those involving populations that were highly spatially proximate,
394 indicating significant genetic differentiation between populations (Suppl. Table 4). PCA revealed
395 three strongly separated population genetic clusters (Figure 1b), but also suggested a high degree
396 of identifiability of individuals from most populations. The first two principal components
397 accounted for 16.75 and 13.27% of the variation. One cluster grouped the eastern populations (AH,
398 AS, BM, FR, SC) and the HO population, the second cluster grouped the western populations (BV,
399 GB, JC, LV, MD, PL, PT, SS, and VM), and lastly, the third cluster grouped EW and DH. The
400 UMAP analyses revealed a striking fine-scale population genetic structure in which all individuals
401 for each population clustered tightly together (note that the distances among UMAP clusters do
402 not represent genetic differentiation among them; Figure 1c). UMAP analyses across the ranges of
403 the minimum distance (MD) and the number of nearest neighbors (NN) parameters also produced
404 generally consistent clustering patterns (Suppl. Figures 2a-h).

405 `ADMIXTURE` identified $K = 8$ as the most likely number of clusters among the 17 populations
406 sampled (Figure 1d), based on cross-validation error values (Suppl. Figure 3). Ancestry coefficient
407 estimates for this analysis produced a similar pattern to the PCA and the UMAP results. Eastern
408 populations formed an ancestry cluster (AH, AS, BM, FR, and SC), while western populations
409 split into two different ancestry clusters (GB, JC, MD, and SS, in one, and PL, PT, and VM, in
410 another). Lastly, the BV, DH, EW, HO, and LV populations were assigned to additional single
411 clusters, reflecting relatively stronger differentiation of these populations in relation to those within
412 the larger ancestral clusters above. Notably, populations from individual seed zones of Johnson et
413 al. (2017) were commonly assigned to multiple ancestral groups in the `ADMIXTURE` results (Figure
414 1d, e.g., populations in seed zones represented by circles belong to three different ancestry groups),
415 illustrating discordance among evolutionary history and seed zones delineated with phenotype-
416 environment associations. The two other most likely K values, $K = 9$ and $K = 10$, generated similar
417 patterns of cluster membership and similar discordance among seed zones and ancestry (see Suppl.
418 Figure 3b).

419 The EEMS results suggested effective migration patterns congruent with previous results.
420 Some populations were connected by higher migration rates (m) than expected under isolation by
421 distance. For example, HO and AH, while separated by approximately 350 km, were connected
422 with high effective migration (Figure 1, Figures 3b, c). Moreover, other groups of populations
423 seem to have resistance barriers to gene flow despite being highly proximate geographically
424 (Figure 3b). For example, PL and PT appear to be distinguished by low effective migration rates
425 despite being separated by only 19 km. Results of unPC analyses (Suppl. Table 5) were broadly
426 consistent with those from the EEMS, suggesting the same regions of low and high effective
427 migration (Figure 3c).

428 The maximum likelihood tree in which all main clades yielded branch support higher than
429 99 produced topologies similarly illustrated pronounced population divergence. Similar to the
430 patterns of clustering in PCA and ADMIXTURE analyses above, tree topology resolved four main
431 clades; the eastern populations (AH, AS, BM, FR, and SC) with HO, the BV population, the EW
432 and DH populations, and lastly, the western populations (GB, JC, MD, SS, LV, PL, PT, and VM)
433 (Figures 4a, b). Similar to evidence for population identifiability in UMAP analyses, individuals
434 from the same populations predominantly clustered together in the maximum likelihood tree,
435 further illustrating population differentiation at fine spatial scales. Consistent with ancestry based
436 analyses above, there was no evidence for phylogenetic signal for seed zones ($\lambda = 0.000$);
437 populations from the same seed zones often appeared in multiple distantly related clades (e.g., DH
438 and EW, or PL and VM, Figures 4 a, b).

439 Genetic-environment association analyses

440 The pool of environmental variables was reduced from 46 to 8 after removing highly
441 correlated variables (based on Pearson's $|r| \leq 0.60$; note that the environmental variables used for
442 seed zone delineation in Johnson et al. (2017), were not included in the analyses to control for
443 multicollinearity, but some of them were correlated with the eight variables selected from our
444 analyses see Suppl. Table 2c). Results from the pRDA provided evidence that specific
445 environmental variables may influence spatial patterns of genetic variation. In particular, the
446 climatic variables explained 23% of the total genetic variation (39% of the variance explained by
447 the full model), suggesting an association between genetic variation and environmental gradients
448 (IBE) (Table 4). The environmental variables with the greatest explained variance in the pRDA
449 were the magnitude of climate water deficit (MaxCWD; 21.01 %, $p < 0.001$) and the folded aspect
450 (AfRad; 17.80 %, $p < 0.001$) (Table 2; Figure 5). The first two constrained axes were significant

451 ($p < 0.001$), explaining 24.63 % and 23.44 % of the total variation (Figure 5). We identified ten
452 loci across the environmental variables associated with the second and third RDA axes (Suppl.
453 Table 2d). Four of these ten loci were associated with the difference between water supply and
454 actual evapotranspiration during the spring (WsAETspr), two with the maximum temperature
455 during the winter season (mxtmpwin), and the four remaining were associated with the cumulative
456 annual actual evapotranspiration during the growing season (AETgdd), the difference between
457 actual evapotranspiration summer low and fall peak (FallAET), the magnitude of climatic water
458 deficit (MaxCWD), and the slope (SlopRad). One of the variables strongly associated with genetic
459 variation the maximum temperature during the winter season (mxtmpwin; Table 2) was highly
460 correlated with the mean average temperature (MAT; Pearson's $|r| = 0.82$), which was among the
461 variables most strongly predicting genecological variation in Johnson et al. (2017).

462 Discussion

463 Understanding the nature of genetic variation in native plants is crucial not only for understanding
464 the origin and maintenance of diversity but also for conserving and restoring populations. Our
465 analyses of population genetic variation in Thurber's needlegrass (*Achnatherum thurberianum*), a
466 widespread bunchgrass in the Great Basin, illustrated strong regional differentiation as well as
467 remarkably fine-scale spatial genetic structure among populations. These patterns, along with low
468 levels of genetic diversity within populations, high inbreeding coefficients, and elevated linkage
469 disequilibrium, are consistent with self-pollination reducing genetic diversity and contributing to
470 spatial genetic structure. Despite low genetic diversity within the sampled populations, our
471 analyses indicated that environmental variation has shaped spatial genetic structure and influenced
472 local adaptation across *A. thurberianum* populations. Our results suggested the potential for local
473 adaptation driven particularly by climate water deficit, aspect, and summer precipitation. Notably,

474 our results illustrated previously unidentified differences in evolutionary history within seed zones
475 proposed for *A. thurberianum* based on phenotype-environment associations (Johnson et al. 2017).
476 Altogether, our results suggest that numerous factors have shaped the spatial genetic structure of
477 *A. thurberianum* across fine geographic and environmental scales and provide baseline
478 information that may be of value for restoration, including allowing managers to consider both
479 phenotypic variation and evolutionary history when making seed source decisions.

480 Strongly congruent results across multiple analyses (F_{ST} , PCA, ADMIXTURE, phylogenomic
481 analyses, AMOVA, and UMAP) illustrated spatial genomic structure across both broad geographic
482 regions and among proximate populations at finer scales than might otherwise be expected for a
483 primarily wind-dispersed species (Linder et al., 2018). For example, at broad regional scales, our
484 analyses consistently illustrated pronounced differentiation among eastern and western groups of
485 populations (Figures 1, 4) including differentiation of two populations at the southwestern limit of
486 sampling. Interestingly, the HO population clustered within the eastern populations, despite being
487 geographically distant and in closer proximity to populations in the northwestern portion of the
488 sampled area (e.g., JC; see Figures 1a, b). These broad patterns of regional differentiation could
489 be explained by historical habitat contractions during the multiple Pleistocene glacial cycles that
490 shaped the Great Basin landscape (Beck and Jones, 1997). In particular, during the Last Glacial
491 Maximum and throughout the last deglaciation, the Great Basin region was marked by the
492 formation of multiple extensive lacustrine systems (Tchakerian and Lancaster, 2002; Lyle et al.,
493 2012), which would have reduced the availability of suitable habitat for *A. thurberianum*. More
494 specifically, a large portion of our study area was historically occupied by Lake Lahontan (38.75–
495 40.75°N, 117.5–120.5°W; Russell, 1885; Matsubara and Howard, 2009), which may have played
496 a central role in shaping regional patterns of marked differentiation in Thurber's needlegrass.

497 Consistent with such history, estimates of effective migration (EEMS and unPC) indicated barriers
498 to gene flow among eastern and western groups of populations, which continue to be separated by
499 low-elevation playas that are inhospitable to this plant (Figures 3b, c). Further, positive values of
500 Tajima's D for each population indicated past population contraction (Table 1; Tajima, 1989).
501 Temperate grass species of Europe (Hensen et al., 2010; Blanco-Pastor et al., 2019; Blanco-Pastor
502 et al., 2021), Africa (Mairal et al., 2021), and North America (Avendaño-González et al., 2019;
503 Palacio-Mejía et al., 2021) demonstrate comparable regional patterns of differentiation and gene
504 flow also influenced by Pleistocene glacial cycles.

505 In addition to the larger-scale geographic patterns, genetic differentiation across smaller
506 geographic scales was evident in phylogenetic analyses, where individuals clustered largely by
507 population, and in the UMAP analyses, where individuals formed population-specific clusters
508 (Figure 1c). UMAP analyses provided remarkable resolution of spatial genetic structure, with all
509 *A. thurberianum* individuals having 100% identifiability to their population of origin. While
510 parameter settings can influence the UMAP depiction of clustering (MD and NN; Diaz-Papkovich
511 et al., 2021), our analyses across a range of two parameters produced largely congruent results
512 with minor variation in the strength of clustering (Suppl. Figure 2). These results suggest that the
513 degree of differentiation among populations seen here could possibly be used to retroactively
514 identify the constituents of historically seeded populations with a high degree of certainty.
515 Estimates of effective migration (EEMS and unPC) also appeared strongly reduced among a
516 number of geographically proximate populations (PT and DH separated by 58 km, or EW and FR
517 separated by 127 km, for example, Figures 3b, c). While gene flow among spatially proximate
518 populations can be high in some wind-dispersed grasses (Vogel et al., 2009; Stritt et al., 2022),
519 pronounced spatial genetic structure has also been reported in Eurasian species of Stipeae (Wagner

520 et al., 2011; Durka et al., 2013). Patterns of population differentiation and identifiability across
521 both large and small geographic scales indicates that genetic variation in *A. thurberianum* has been
522 shaped by a combination of historical isolation, local adaptation to environment, as well as life
523 history variation.

524 Species that rely strongly on self-fertilization cannot maintain high levels of genetic
525 diversity within populations through frequent pollen movement and therefore tend to have low
526 genetic diversity (Hamrick and Godt, 1996; Honnay and Jacquemyn, 2007; Durka et al., 2013;
527 Huang et al., 2021). Moreover, selfing plant species can be prone to developing fine-scale spatial
528 genetic structure due to reduction in effective population sizes and effective migration (Volis et
529 al., 2010; Huang et al., 2021). The populations studied here were characterized by low levels of
530 genetic diversity (mean H_e : 0.04; mean H_o : 0.02; mean π : 0.05), strongly positive inbreeding
531 coefficient estimates (F_{IS}), and a high degree of linkage disequilibrium (r_d^- and I_A) (Table 1), all
532 of which are consistent with a mating system dominated by self-fertilization. While studies directly
533 assessing the mating system of *A. thurberianum* are lacking, many closely related species from the
534 Poaceae family have been described as self-fertilized (Jones and Nielson, 1989; Arnesen et al.,
535 2017; Marques et al., 2017; Stritt et al. 2022). Indeed, grass species employing self-fertilization
536 have been commonly documented to have low genetic diversity and pronounced spatial genetic
537 structure (Dell'Acqua et al., 2014; Marques et al., 2017; Guo et al., 2017), presumably due to small
538 effective population sizes and genetic drift in the absence of much gene flow. Our results suggest
539 high rates of self-fertilization in *A. thurberianum* have likely contributed to its pronounced spatial
540 genetic structure in the western Great Basin.

541 Although mating system and low genetic diversity have allowed genetic drift to influence
542 spatial genetic structure, environmental variation also appears to have contributed to genetic

543 variation in *A. thurberianum*. The environmental variables influencing spatial genetic variation in
544 *A. thurberianum* are known to predict genetic and phenotypic variation across populations of other
545 plant species (Dilts et al., 2015; Barga et al., 2018; Faske et al., 2021) and have been commonly
546 implicated as underlying local adaptation in genecological studies of Great Basin plant species
547 (Johnson et al. 2017; Baughman et al., 2019). Variance partitioning with partial RDA illustrated
548 that neutral genetic structure, geography, and environmental variation together explained a
549 substantial proportion of genetic variance (Table 4). However, the individual contribution of
550 environmental variation was substantially stronger than that of both genetic structure and
551 geography (Table 4). Variation in environmental variables (Table 2), especially climate water
552 deficit, aspect, and summer precipitation, explained a substantial proportion of genetic variation
553 and influenced spatial genetic structure (Table 2, Figure 5). The pronounced environmental
554 heterogeneity of the Great Basin (Figure 2c) could commonly give rise to Isolation by
555 Environment (IBE), where environmental transitions act as barriers to gene flow or where local
556 adaptation to different environments leads to low migrant fitness (Shafer and Wolf, 2013; Wang
557 and Bradburd, 2014). Genomic evidence for environment contributing to spatial genetic structure
558 and perhaps local adaptation is consistent with results from a common garden study of phenotypic
559 variation across 66 Great Basin *A. thurberianum* populations that inferred local adaptation to
560 environment as a basis for delineating seed zones (Johnson et al. 2017).

561 Given the strong influence of environmental variables on genetic variation observed here
562 and in Johnson et al. (2017), along with the topographically and environmentally heterogeneous
563 nature of this region, we suspected that proposed seed zones might span populations from distantly
564 related clades. Indeed, geographically differentiated groups of populations commonly crossed
565 multiple seed zones, and specific seed zones were represented across distantly related clades

566 (Figures 1, 4). It is worth noting that our sampling focused on an area that was not well represented
567 in the sampling design for the phenotype-based seed zone development (Johnson et al. 2017),
568 which might indicate that caution is warranted when designating seed zones outside areas of
569 extensive sampling. Convergent evolution, or adaptation to parallel environmental conditions
570 across divergent lineages, is well documented across diverse groups of plants (e.g., Rellstab et al.
571 2020; Xu et al. 2020), and this possibility should be considered for seed zone design in the Great
572 Basin, especially if particular geographic regions show consistent barriers to gene flow for multiple
573 species. Indeed, other plant species from the Great Basin have been found to have similar patterns
574 of population genetic structure in the vicinity of historic Lake Lahontan (e.g., Faske et al., 2021).
575 Convergent evolution could have consequences for restoration if outbreeding depression
576 (reviewed in Edmands, 2007) or genetic incompatibilities (Etterson et al. 2007) occur in seed
577 mixes containing distantly related populations delineated as part of a single seed zone.

578 In addition to its relevance for seed zones, a general understanding of genetic diversity,
579 population differentiation, and local adaptation in *A. thurberianum* could have utility for guiding
580 ecological restoration (Mijangos et al., 2015; Breed et al., 2019). Populations exhibited very low
581 levels of standing variation, presumably due to high self-fertilization rates, which likely
582 contributed to population differentiation at such fine spatial scales. Low diversity can be a concern
583 when sourcing seeds for restoration, as genetic diversity is often viewed as a proxy for evolutionary
584 potential (Ellstrand and Elam, 1993), and some have proposed mixing populations of low-diversity
585 species as a way to increase the chances of long-term persistence of restored populations (Bischoff
586 et al., 2010; Bucharova et al., 2019; St. Clair et al., 2020). While this may lead to risks of
587 outbreeding depression in some species, this might be reduced for highly-selfing species like *A.*
588 *thurberianum* (Jones and Nielson, 1989). Despite very low diversity, our analyses indicated that

589 environmental variation has shaped spatial genetic structure and influenced local adaptation
590 across *A. thurberianum* populations of the Great Basin. Generally, consistent results of inference
591 of local adaptation in our study with that from phenotypic analyses of genecological experiments
592 (Johnson et al., 2017; Baughman et al., 2019) highlight the utility of population genomic analyses
593 for characterizing the environmental variables contributing to local adaptation while additionally
594 characterizing levels of diversity and differentiation across space, all of which have value for
595 guiding provenance and seed sourcing (Breed et al., 2019; Rossetto et al., 2019).

596 **Data Archiving Statement**

597 The trimmed vcf file and scripts used for analyses can be found at the Dryad Digital Repository:
598 <https://doi.org/10.5061/dryad.pvmcvdnpn>. The raw data from this project were submitted to NCBI
599 Sequence Read Archive (SRA) and can be found by the BioProject ID PRJNA849003. The
600 individual fastq files for each population can be found under the following accession numbers: AH
601 (SRR19646741), AS (SRR19646740), BM (SRR19646732), BV (SRR19646731), DH
602 (SRR19646730), EW (SRR19646729), FR (SRR19646728), GB (SRR19646727), HO
603 (SRR19646726), JC (SRR19646725), LV (SRR19646739), MD (SRR19646738), PL
604 (SRR19646737), PT (SRR19646736), SC (SRR19646735), SS (SRR19646734), VM
605 (SRR19646733).

606

607 **Acknowledgments:** The authors thank Fred Edwards, Trevor Faske, Joshua Hallas, Katie Uckele,
608 and Joshua P. Jahner for helpful discussion in support of project design and analyses. Owen
609 Baughman, Lana Sheta, Sage Ellis, and Meagan O'Farrell assisted with the collection of plant
610 material. This work was supported by funding from the U.S. Department of Agriculture (Award
611 Number: 2017-67019-26336) and the U.S. Bureau of Land Management (Award Numbers:
612 L16AC00318 and L19AC00013).

613

614

615

616

617

618

619 **Literature cited**

- 620
- 621 Agneray, A., Parchman, T., Leger, E. (2022). Phenotypic traits and environment strongly predict
622 seedling survival for seven co-occurring Great Basin plant taxa growing with invasive
623 grass. *Ecology and Evolution*, 12 (5), e8870.
- 624 Alexander, D. H., & Lange, K. (2011). Enhancements to the ADMIXTURE algorithm for
625 individual ancestry estimation. *BMC Bioinformatics*, 12 (1), 1-6.
- 626 Alvarez, N., Thiel-Egenter, C., Tribsch, A., Holderegger, R., Manel, S., Schönswetter, P., ... &
627 IntraBioDiv Consortium. (2009). History or ecology? Substrate type as a major driver of
628 spatial genetic structure in Alpine plants. *Ecology Letters*, 12 (7), 632-640.
- 629 Andrews, K. R., Good, J. M., Miller, M. R., Luikart, G., & Hohenlohe, P. A. (2016). Harnessing
630 the power of RADseq for ecological and evolutionary genomics. *Nature Reviews Genetics*,
631 17 (2), 81-92.
- 632 Arnesen, S., Coleman, C. E., & Meyer, S. E. (2017). Population genetic structure of *Bromus*
633 *tectorum* in the mountains of western North America. *American Journal of Botany*, 104
634 (6), 879-890.
- 635 Avendaño-González, M., Morales-Domínguez, J. F., & Siqueiros-Delgado, M. E. (2019). Genetic
636 structure, phylogeography, and migration routes of *Bouteloua gracilis* (Kunth) Lag. ex
637 Griffiths (Poaceae: Chloridoideae). *Molecular Phylogenetics and Evolution*, 134, 50-60.
- 638 Balch, J. K., Bradley, B. A., D'Antonio, C. M., & Gómez-Dans, J. (2013). Introduced annual grass
639 increases regional fire activity across the arid western USA (1980–2009). *Global Change
640 Biology*, 19 (1), 173-183.

- 641 Barga, S. C., Dilts, T. E., & Leger, E. A. (2018). Contrasting climate niches among co-occurring
642 subdominant forbs of the sagebrush steppe. *Diversity and Distributions*, 24 (9), 1291-1307.
- 643 Barkworth, M. E. (1993). North American Stipeae (Gramineae): taxonomic changes and other
644 comments. *Phytologia*, 74 (1), 1-25.
- 645 Bauert, M. R., Kälin, M., Baltisberger, M., & Edwards, P. J. (1998). No genetic variation detected
646 within isolated relict populations of *Saxifraga cernua* in the Alps using RAPD
647 markers. *Molecular Ecology*, 7 (11), 1519-1527.
- 648 Baughman, O. W., Agneray, A. C., Forister, M. L., Kilkenny, F. F., Espeland, E. K., Fiegner, R.,
649 Horning, M. E., & Leger, E. A. (2019). Strong patterns of intraspecific variation and local
650 adaptation in Great Basin plants revealed through a review of 75 years of
651 experiments. *Ecology and Evolution*, 9 (11), 6259-6275.
- 652 Beck, C., & Jones, G. T. (1997). The terminal Pleistocene/early Holocene archaeology of the Great
653 Basin. *Journal of World Prehistory*, 11 (2), 161-236.
- 654 Bischoff, A., Steinger, T., & Müller-Schärer, H. (2010). The importance of plant provenance and
655 genotypic diversity of seed material used for ecological restoration. *Restoration Ecology*,
656 18 (3), 338-348.
- 657 Blanco-Pastor, J. L., Manel, S., Barre, P., Roschanski, A. M., Willner, E., Dehmer, K. J., Hegarty,
658 M., Muylle, H., Ruttink, T., Roldán-Ruiz, I., & Sampoux, J. P. (2019). Pleistocene climate
659 changes, and not agricultural spread, accounts for range expansion and admixture in the
660 dominant grassland species *Lolium perenne* L. *Journal of Biogeography*, 46 (7), 1451-
661 1465.

- 662 Blanco-Pastor, J. L., Barre, P., Keep, T., Ledauphin, T., Escobar-Gutiérrez, A., Roschanski, A. M.,
663 ... & Sampoux, J. P. (2021). Canonical correlations reveal adaptive loci and phenotypic
664 responses to climate in perennial ryegrass. *Molecular Ecology Resources*, 21 (3), 849-870.
- 665 Booy, G., Hendriks, R. J. J., Smulders, M. J. M., Van Groenendaal, J. M., & Vosman, B. (2000).
666 Genetic diversity and the survival of populations. *Plant Biology*, 2 (04), 379-395.
- 667 Breed, M. F., Harrison, P. A., Blyth, C., Byrne, M., Gaget, V., Gellie, N. J., ... & Mohr, J. J. (2019).
668 The potential of genomics for restoring ecosystems and biodiversity. *Nature Reviews Genetics*,
669 20 (10), 615-628.
- 670 Brown, A. H. D., Feldman, M. W., & Nevo, E. (1980). Multilocus structure of natural populations
671 of *Hordeum spontaneum*. *Genetics*, 96 (2), 523-536.
- 672 Bucharova, A., Bossdorf, O., Hözel, N., Kollmann, J., Prasse, R., & Durka, W. (2019). Mix and
673 match: regional admixture provenancing strikes a balance among different seed-sourcing
674 strategies for ecological restoration. *Conservation Genetics*, 20 (1), 7-17.
- 675 Capblancq, T., & Forester, B. R. (2021). Redundancy analysis: A Swiss Army Knife for landscape
676 genomics. *Methods in Ecology and Evolution*, 12 (12), 2298-2309.
- 677 Capella-Gutiérrez, S., Silla-Martínez, J. M., & Gabaldón, T. (2009). trimAl: a tool for automated
678 alignment trimming in large-scale phylogenetic analyses. *Bioinformatics*, 25 (15), 1972-
679 1973.
- 680 Carvalho, C. S., Forester, B. R., Mitre, S. K., Alves, R., Imperatriz-Fonseca, V. L., Ramos, S. J.,
681 ... & Jaffé, R. (2021). Combining genotype, phenotype, and environmental data to delineate
682 site-adjusted provenance strategies for ecological restoration. *Molecular Ecology Resources*,
683 21 (1), 44-58.

- 684 Catchen, J. M., Amores, A., Hohenlohe, P., Cresko, W., & Postlethwait, J. H. (2011). Stacks:
685 building and genotyping loci de novo from short-read sequences. *G3: Genes|genomes|*
686 *genetics*, 1(3), 171-182.
- 687 Catchen, J., Hohenlohe, P. A., Bassham, S., Amores, A., & Cresko, W. A. (2013). Stacks: an
688 analysis tool set for population genomics. *Molecular Ecology*, 22 (11), 3124-3140.
- 689 Chambers, J. C., & Wisdom, M. J. (2009). Priority research and management issues for the
690 imperiled Great Basin of the western United States. *Restoration Ecology*, 17 (5), 707-714.
- 691 Cialdella, A. M., Salariato, D. L., Aagesen, L., Giussani, L. M., Zuloaga, F. O., & Morrone, O.
692 (2010). Phylogeny of New World Stipeae (Poaceae): an evaluation of the monophyly of
693 *Aciachne* and *Amelichloa*. *Cladistics*, 26 (6), 563-578.
- 694 Danecek, P., Auton, A., Abecasis, G., Albers, C. A., Banks, E., DePristo, M. A., ... & 1000
695 Genomes Project Analysis Group. (2011). The variant call format and
696 VCFtools. *Bioinformatics*, 27 (15), 2156-2158.
- 697 Dell'Acqua, M., Zuccolo, A., Tuna, M., Gianfranceschi, L., & Pè, M. E. (2014). Targeting
698 environmental adaptation in the monocot model *Brachypodium distachyon*: a multi-faceted
699 approach. *BMC Genomics*, 15 (1), 1-17.
- 700 Diaz-Papkovich, A., Anderson-Trocmé, L., Ben-Eghan, C., & Gravel, S. (2019). UMAP reveals
701 cryptic population structure and phenotype heterogeneity in large genomic cohorts. *PLoS*
702 *Genetics*, 15 (11), e1008432.
- 703 Diaz-Papkovich, A., Anderson-Trocmé, L., & Gravel, S. (2021). A review of UMAP in
704 population genetics. *Journal of Human Genetics*, 66 (1), 85-91.

- 705 Dilts, T. E., Weisberg, P. J., Dencker, C. M., & Chambers, J. C. (2015). Functionally relevant
706 climate variables for arid lands: a climatic water deficit approach for modelling desert
707 shrub distributions. *Journal of Biogeography*, 42 (10), 1986-1997.
- 708 Dudley, N., Eufemia, L., Fleckenstein, M., Periago, M. E., Petersen, I., & Timmers, J. F. (2020).
709 Grasslands and savannahs in the UN Decade on Ecosystem Restoration. *Restoration
710 Ecology*, 28 (6), 1313-1317.
- 711 Duminil, J., Fineschi, S., Hampe, A., Jordano, P., Salvini, D., Vendramin, G. G., & Petit, R. J.
712 (2007). Can population genetic structure be predicted from life-history traits?. *The
713 American Naturalist*, 169 (5), 662-672.
- 714 Durka, W., Nossol, C., Welk, E., Ruprecht, E., Wagner, V., Wesche, K., & Hensen, I. (2013).
715 Extreme genetic depauperation and differentiation of both populations and species in
716 Eurasian feather grasses (*Stipa*). *Plant Systematics and Evolution*, 299 (1), 259-269.
- 717 Edmands, S. (2007). Between a rock and a hard place: evaluating the relative risks of inbreeding
718 and outbreeding for conservation and management. *Molecular Ecology*, 16 (3), 463-475.
- 719 Ellstrand, N. C., & Elam, D. R. (1993). Population genetic consequences of small population size:
720 implications for plant conservation. *Annual review of Ecology and Systematics*, 24 (1),
721 217-242.
- 722 Etterson, J. R., Keller, S. R., & Galloway, L. F. (2007). Epistatic and cytonuclear interactions
723 govern outbreeding depression in the autotetraploid *Campanulastrum americanum*.
724 *Evolution: International Journal of Organic Evolution*, 61 (11), 2671-2683.
- 725 Faske, T. M., Agneray, A. C., Jahner, J. P., Sheta, L. M., Leger, E. A., & Parchman, T. L. (2021).
726 Genomic and common garden approaches yield complementary results for quantifying

- 727 environmental drivers of local adaptation in rubber rabbitbrush, a foundational Great Basin
728 shrub. *Evolutionary Applications*, 14 (12), 2881-2900.
- 729 Forester, B. R., Lasky, J. R., Wagner, H. H., & Urban, D. L. (2018). Comparing methods for
730 detecting multilocus adaptation with multivariate genotype–environment
731 associations. *Molecular Ecology*, 27 (9), 2215-2233.
- 732 Gamba, D., & Muchhal, N. (2020). Global patterns of population genetic differentiation in seed
733 plants. *Molecular Ecology*, 29 (18), 3413-3428.
- 734 Gao, S. B., Mo, L. D., Zhang, L. H., Zhang, J. L., Wu, J. B., Wang, J. L., ... & Gao, Y. B. (2018).
735 Phenotypic plasticity vs. local adaptation in quantitative traits differences of *Stipa grandis*
736 in semi-arid steppe, China. *Scientific Reports*, 8 (1), 1-8.
- 737 Gavrilets, S., Li, H., & Vose, M. D. (2000). Patterns of parapatric speciation. *Evolution*, 54 (4),
738 1126-1134.
- 739 Goudet, J. (2005). Hierfstat, a package for R to compute and test hierarchical F-
740 statistics. *Molecular Ecology Notes*, 5 (1), 184-186.
- 741 Guo, C., Ma, L., Yuan, S., & Wang, R. (2017). Morphological, physiological and anatomical traits
742 of plant functional types in temperate grasslands along a large-scale aridity gradient in
743 northeastern China. *Scientific Reports*, 7 (1), 1-10.
- 744 Hamasha, H. R., von Hagen, K. B., & Röser, M. (2012). *Stipa* (Poaceae) and allies in the Old
745 World: molecular phylogenetics realigns genus circumscription and gives evidence on the
746 origin of American and Australian lineages. *Plant Systematics and Evolution*, 298 (2), 351-
747 367.

- 748 Hamasha, H. R., Schmidt-Lebuhn, A. N., Durka, W., Schleuning, M., & Hensen, I. (2013).
- 749 Bioclimatic regions influence genetic structure of four Jordanian *Stipa* species. *Plant*
750 *Biology*, 15 (5), 882-891.
- 751 Hamrick, J. L., & Godt, M. W. (1996). Effects of life history traits on genetic diversity in plant
752 species. *Philosophical Transactions of the Royal Society of London. Series B: Biological*
753 *Sciences*, 351 (1345), 1291-1298.
- 754 Harmon, L., Weir, J., Brock, C., Glor, R., Challenger, W., Hunt, G., ... & Rcpp, L. (2015). Package
755 ‘geiger’. R package version, 2 (3).
- 756 Hart, E., Bell, K., & Butler, A. (2015). PRISM: Access Data From the Oregon State PRISM
757 Climate Project. *Genève: Zenodo*.
- 758 Hedrick, P. (2005). Genetic restoration:'a more comprehensive perspective than 'genetic
759 rescue. *Trends in Ecology & Evolution*, 20 (3), 109.
- 760 Hensen, I., Kilian, C., Wagner, V., Durka, W., Pusch, J., & Wesche, K. (2010). Low genetic
761 variability and strong differentiation among isolated populations of the rare steppe grass
762 *Stipa capillata* L. in central Europe. *Plant Biology*, 12 (3), 526-536.
- 763 Hijmans, R. J., Williams, E., Vennes, C., & Hijmans, M. R. J. (2017). Package
764 ‘geosphere’. *Spherical Trigonometry*, 1 (7).
- 765 Hohenlohe, P. A., Funk, W. C., & Rajora, O. P. (2021). Population genomics for wildlife
766 conservation and management. *Molecular Ecology*, 30 (1), 62-82.
- 767 Holderegger, R., & Wagner, H. H. (2008). Landscape genetics. *Bioscience*, 58 (3), 199-207.
- 768 Holderegger, R., Buehler, D., Gugerli, F., & Manel, S. (2010). Landscape genetics of
769 plants. *Trends in Plant Science*, 15 (12), 675-683.

- 770 Hollister, J., & Shah, T. (2017). elevatr: access elevation data from various APIs. *http://github.com/usepa/elevatr*.
- 772 Holsinger, K. E. (2000). Reproductive systems and evolution in vascular plants. *Proceedings of the National Academy of Sciences*, 97 (13), 7037-7042.
- 774 Honnay, O., & Jacquemyn, H. (2007). Susceptibility of common and rare plant species to the genetic consequences of habitat fragmentation. *Conservation Biology*, 21 (3), 823-831.
- 776 Hoskin, C. J., Higgle, M., McDonald, K. R., & Moritz, C. (2005). Reinforcement drives rapid allopatric speciation. *Nature*, 437 (7063), 1353-1356.
- 778 House, G. L., & Hahn, M. W. (2018). Evaluating methods to visualize patterns of genetic differentiation on a landscape. *Molecular Ecology Resources*, 18 (3), 448-460.
- 780 Huang, R., Zhang, Z. D., Wang, Y., & Wang, Y. Q. (2021). Genetic variation and genetic structure within metapopulations of two closely related selfing and outcrossing Zingiber species (Zingiberaceae). *AoB Plants*, 13 (1), plaa065.
- 783 Hufford, K. M., & Mazer, S. J. (2003). Plant ecotypes: genetic differentiation in the age of ecological restoration. *Trends in Ecology & Evolution*, 18 (3), 147-155.
- 785 Hufford, K. M., Krauss, S. L., & Veneklaas, E. J. (2012). Inbreeding and outbreeding depression in *Stylidium hispidum*: implications for mixing seed sources for ecological restoration. *Ecology and Evolution*, 2 (9), 2262-2273.
- 788 Jacobs, S., Bayer, R., Everett, J., Arriaga, M., Barkworth, M., Sabin-Badereau, A., ... & Bagnall, N. (2007). Systematics of the tribe Stipeae (Gramineae) using molecular data. *Aliso: A Journal of Systematic and Evolutionary Botany*, 23 (1), 349-361.

- 791 Johnson, R. C., Leger, E. A., & Vance-Borland, K. (2017). Genecology of Thurber's Needlegrass
792 (*Achnatherum thurberianum* [Piper] Barkworth) in the Western United States. *Rangeland
793 Ecology & Management*, 70 (4), 509-517.
- 794 Jombart, T. (2008). adegenet: a R package for the multivariate analysis of genetic
795 markers. *Bioinformatics*, 24 (11), 1403-1405.
- 796 Jones, T. A., & Nielson, D. C. (1989). Self-compatibility in 'Paloma' Indian ricegrass. *Rangeland
797 Ecology & Management*, 42 (3), 187-190.
- 798 Kamvar, Z. N., Tabima, J. F., & Grünwald, N. J. (2014). Poppr: an R package for genetic analysis
799 of populations with clonal, partially clonal, and/or sexual reproduction. *PeerJ*, 2, e281.
- 800 Kawecki, T. J., & Ebert, D. (2004). Conceptual issues in local adaptation. *Ecology Letters*, 7 (12),
801 1225-1241.
- 802 Knapp, E. E., & Rice, K. J. (1994). Starting from Seed Genetic Issues in Using Native Grasses for
803 Restoration. *Ecological Restoration*, 12 (1), 40-45.
- 804 Knapp, P. A. (1996). Cheatgrass (*Bromus tectorum* L) dominance in the Great Basin
805 Desert: history, persistence, and influences to human activities. *Global Environmental
806 Change*, 6 (1), 37-52.
- 807 Konopka, T. (2020). umap: Uniform Manifold Approximation and Projection. R package version
808 0.2. 5.0.
- 809 Kraehmer, H. (Ed.). (2019). Grasses: Crops, Competitors, and Ornamentals. USA: John Wiley &
810 Sons, Inc.
- 811 Leland, M., John, H., Nathaniel, S., & Lukas, G. (2018). UMAP: uniform manifold approximation
812 and projection. *Journal of Open Source Software*, 3 (29), 861.

- 813 Leger, E. A., Barga, S., Agneray, A. C., Baughman, O., Burton, R., & Williams, M. (2021).
- 814 Selecting native plants for restoration using rapid screening for adaptive traits: methods
815 and outcomes in a Great Basin case study. *Restoration Ecology*, 29 (4), e13260.
- 816 Lewis, P. O. (2001). A likelihood approach to estimating phylogeny from discrete morphological
817 character data. *Systematic Biology*, 50 (6), 913-925.
- 818 Linder, H. P., Lehmann, C. E., Archibald, S., Osborne, C. P., & Richardson, D. M. (2018). Global
819 grass (Poaceae) success underpinned by traits facilitating colonization, persistence and
820 habitat transformation. *Biological Reviews*, 93 (2), 1125-1144.
- 821 Lyle, M., Heusser, L., Ravelo, C., Yamamoto, M., Barron, J., Diffenbaugh, N. S., ... & Andreasen,
822 D. (2012). Out of the tropics: the Pacific, Great Basin Lakes, and Late Pleistocene water
823 cycle in the western United States. *Science*, 337 (6102), 1629-1633.
- 824 Mairal, M., Namaganda, M., Gizaw, A., Chala, D., Brochmann, C., & Catalán, P. (2021). Multiple
825 mountain-hopping colonization of sky-islands on the two sides of Tropical Africa during
826 the Pleistocene: The afroalpine Festuca grasses. *Journal of Biogeography*, 48 (8), 1858-
827 1874.
- 828 Manel, S., Schwartz, M. K., Luikart, G., & Taberlet, P. (2003). Landscape genetics: combining
829 landscape ecology and population genetics. *Trends in Ecology & Evolution*, 18 (4), 189-
830 197.
- 831 Manichaikul, A., Mychaleckyj, J. C., Rich, S. S., Daly, K., Sale, M., & Chen, W. M. (2010). Robust
832 relationship inference in genome-wide association studies. *Bioinformatics*, 26 (22), 2867-
833 2873.
- 834 Marques, I., Shiposha, V., López-Alvarez, D., Manzaneda, A. J., Hernandez, P., Olonova, M., &
835 Catalán, P. (2017). Environmental isolation explains Iberian genetic diversity in the highly

- 836 homozygous model grass *Brachypodium distachyon*. *BMC Evolutionary Biology*, 17(1),
837 1-14.
- 838 Massatti, R., Prendeville, H. R., Larson, S., Richardson, B. A., Waldron, B., & Kilkenny, F. F.
839 (2018). Population history provides foundational knowledge for utilizing and developing
840 native plant restoration materials. *Evolutionary Applications*, 11 (10), 2025-2039.
- 841 Mastretta-Yanes, A., Arrigo, N., Alvarez, N., Jorgensen, T. H., Piñero, D., & Emerson, B. C.
842 (2015). Restriction site-associated DNA sequencing, genotyping error estimation and de
843 novo assembly optimization for population genetic inference. *Molecular Ecology*
844 *Resources*, 15 (1), 28-41.
- 845 Matsubara, Y., & Howard, A. D. (2009). A spatially explicit model of runoff, evaporation, and
846 lake extent: Application to modern and late Pleistocene lakes in the Great Basin region,
847 western United States. *Water Resources Research*, 45 (6).
- 848 McInnes, L., Healy, J., & Melville, J. (2018). Umap: Uniform manifold approximation and
849 projection for dimension reduction. *arXiv:1802.03426*.
- 850 McKay, J. K., Christian, C. E., Harrison, S., & Rice, K. J. (2005). “How local is local?”—a review
851 of practical and conceptual issues in the genetics of restoration. *Restoration Ecology*, 13
852 (3), 432-440.
- 853 Mijangos, J. L., Pacioni, C., Spencer, P. B., & Craig, M. D. (2015). Contribution of genetics to
854 ecological restoration. *Molecular Ecology*, 24 (1), 22-37.
- 855 Mosca, E., Di Pierro, E. A., Budde, K. B., Neale, D. B., & González-Martínez, S. C. (2018).
856 Environmental effects on fine-scale spatial genetic structure in four Alpine keystone forest
857 tree species. *Molecular Ecology*, 27 (3), 647-658.

- 858 Nagy, R. C., Fusco, E. J., Balch, J. K., Finn, J. T., Mahood, A., Allen, J. M., & Bradley, B. A.
859 (2021). A synthesis of the effects of cheatgrass invasion on US Great Basin carbon
860 storage. *Journal of Applied Ecology*, 58 (2), 327-337.
- 861 Nei, M. (1987). Evolutionary change of amino acid sequences. *Molecular Evolutionary*
862 *Genetics* (pp. 39-63). New York: Columbia University Press.
- 863 Nguyen, L. T., Schmidt, H. A., Von Haeseler, A., & Minh, B. Q. (2015). IQ-TREE: a fast and
864 effective stochastic algorithm for estimating maximum-likelihood phylogenies. *Molecular*
865 *Biology and Evolution*, 32 (1), 268-274.
- 866 Oksanen, J., Blanchet, F. G., Kindt, R., Legendre, P., Minchin, P. R., O'hara, R. B., ... & Oksanen,
867 M. J. (2013). Package ‘vegan’. Community ecology package, version, 2 (9), 1-295.
- 868 Orsini, L., Vanoverbeke, J., Swillen, I., Mergeay, J., & De Meester, L. (2013). Drivers of
869 population genetic differentiation in the wild: isolation by dispersal limitation, isolation by
870 adaptation and isolation by colonization. *Molecular Ecology*, 22 (24), 5983-5999.
- 871 Ortego, J., Riordan, E. C., Gugger, P. F., & Sork, V. L. (2012). Influence of environmental
872 heterogeneity on genetic diversity and structure in an endemic southern Californian
873 oak. *Molecular Ecology*, 21 (13), 3210-3223.
- 874 Ortiz, E. M. (2019). vcf2phylip v2. 0: convert a VCF matrix into several matrix formats for
875 phylogenetic analysis. *Zenodo*. 2.0.
- 876 Ottewell, K. M., Bickerton, D. C., Byrne, M., & Lowe, A. J. (2016). Bridging the gap: a genetic
877 assessment framework for population-level threatened plant conservation prioritization and
878 decision-making. *Diversity and Distributions*, 22 (2), 174-188.
- 879 Pagel, M. (1999). Inferring the historical patterns of biological evolution. *Nature*, 401:877–884.

- 880 Palacio-Mejía, J. D., Grabowski, P. P., Ortiz, E. M., Silva-Arias, G. A., Haque, T., Des Marais, D.
881 L., ... & Juenger, T. E. (2021). Geographic patterns of genomic diversity and structure in
882 the C4 grass *Panicum hallii* across its natural distribution. *AoB Plants*, 13 (2), plab002..
883 Paradis, E., Claude, J., & Strimmer, K. (2004). APE: analyses of phylogenetics and evolution in
884 R language. *Bioinformatics*, 20 (2), 289-290.
885 Parchman, T. L., Gompert, Z., Mudge, J., Schilkey, F. D., Benkman, C. W., & Buerkle, C. A.
886 (2012). Genome-wide association genetics of an adaptive trait in lodgepole
887 pine. *Molecular Ecology*, 21 (12), 2991-3005.
888 Paris, J. R., Stevens, J. R., & Catchen, J. M. (2017). Lost in parameter space: a road map for
889 stacks. *Methods in Ecology and Evolution*, 8 (10), 1360-1373.
890 Parkinson, H., Zabinski, C., & Shaw, N. (2013). Impact of native grasses and cheatgrass (*Bromus*
891 *tectorum*) on Great Basin forb seedling growth. *Rangeland Ecology & Management*, 66
892 (2), 174-180.
893 Patterson, N., Price, A. L., & Reich, D. (2006). Population structure and eigenanalysis. *PLoS
894 Genetics*, 2 (12), e190.
895 Paz, A., Ibáñez, R., Lips, K. R., & Crawford, A. J. (2015). Testing the role of ecology and life
896 history in structuring genetic variation across a landscape: A trait-based phylogeographic
897 approach. *Molecular Ecology*, 24 (14), 3723-3737.
898 Pedlar, J. H., McKenney, D. W., & Lu, P. (2021). Critical seed transfer distances for selected tree
899 species in eastern North America. *Journal of Ecology*, 109 (6), 2271-2283.
900 Peterson, B. K., Weber, J. N., Kay, E. H., Fisher, H. S., & Hoekstra, H. E. (2012). Double digest
901 RADseq: an inexpensive method for de novo SNP discovery and genotyping in model and
902 non-model species. *PloS One*, 7 (5), e37135.

- 903 Peterson, P. M., Romaschenko, K., Soreng, R. J., & Reyna, J. V. (2019). A key to the North
904 American genera of Stipeae (Poaceae, Pooideae) with descriptions and taxonomic names
905 for species of Eriocoma, Neotrinia, Oloptum, and five new genera: Barkworthia,^x
906 Eriosella, Pseudoeriocoma, Ptilagrostiella, and Thorneochloa. *PhytoKeys*, 126, 89.
- 907 Petkova, D., Novembre, J., & Stephens, M. (2016). Visualizing spatial population structure with
908 estimated effective migration surfaces. *Nature Genetics*, 48 (1), 94-100.
- 909 Pilliod, D. S., & Arkle, R. S. (2013). Performance of quantitative vegetation sampling methods
910 across gradients of cover in Great Basin plant communities. *Rangeland Ecology &*
911 *Management*, 66 (6), 634-647.
- 912 Pilliod, D. S., Welty, J. L., & Toebs, G. R. (2017). Seventy-five years of vegetation
913 treatments on public rangelands in the Great Basin of North America. *Rangelands*, 39 (1),
914 1-9.
- 915 Purcell, S., Neale, B., Todd-Brown, K., Thomas, L., Ferreira, M. A., Bender, D., ... & Sham, P. C.
916 (2007). PLINK: a tool set for whole-genome association and population-based linkage
917 analyses. *The American Journal of Human Genetics*, 81 (3), 559-575.
- 918 Rambaut, A. (2018). FigTree Retrieved from <http://tree.bio.ed.ac.uk/software/figtree>.
- 919 Rellstab, C., Zoller, S., Sailer, C., Tedder, A., Gugerli, F., Shimizu, K. K., ... & Fischer, M. C.
920 (2020). Genomic signatures of convergent adaptation to Alpine environments in three
921 Brassicaceae species. *Molecular Ecology*, 29 (22), 4350-4365.
- 922 Revell, L. J., & Revell, M. L. J. (2014). Package ‘phytools’. Website: <https://cran.r-project.org/web/packages/phytools>.
- 924 Revelle, W., & Revelle, M. W. (2015). Package ‘psych’. *The comprehensive R archive
925 network*, 337, 338.

- 926 Rochette, N. C., Rivera-Colón, A. G., & Catchen, J. M. (2019). Stacks 2: Analytical methods for
927 paired-end sequencing improve RADseq-based population genomics. *Molecular
928 Ecology*, 28 (21), 4737-4754.
- 929 Romaschenko, K., Peterson, P. M., Soreng, R. J., Garcia-Jacas, N., & Susanna, A. (2010).
930 Phylogenetics of Stipeae (Poaceae: Pooideae) based on plastid and nuclear DNA
931 sequences. *Diversity, phylogeny, and evolution in the monocotyledons*.
- 932 Romaschenko, K., Peterson, P. M., Soreng, R. J., Garcia-Jacas, N., Futorna, O., & Susanna, A.
933 (2012). Systematics and evolution of the needle grasses (Poaceae: Pooideae: Stipeae) based
934 on analysis of multiple chloroplast loci, ITS, and lemma micromorphology. *Taxon*, 61 (1),
935 18-44.
- 936 Rossetto, M., Bragg, J., Kilian, A., McPherson, H., van der Merwe, M., & Wilson, P. D. (2019).
937 Restore and renew: A genomics-era framework for species provenance
938 delimitation. *Restoration Ecology*, 27 (3), 538-548.
- 939 Russell, I. C. (1885). Geological history of Lake Lahontan: a Quaternary lake of northwestern
940 Nevada.
- 941 Shackelford, N., Paterno, G. B., Winkler, D. E., Erickson, T. E., Leger, E. A., Svejcar, L. N., ... &
942 Suding, K. L. (2021). Drivers of seedling establishment success in dryland restoration
943 efforts. *Nature Ecology & Evolution*, 5 (9), 1283-1290.
- 944 Schubert, M., Grønvold, L., Sandve, S. R., Hvidsten, T. R., & Fjellheim, S. (2019). Evolution of
945 cold acclimation and its role in niche transition in the temperate grass subfamily
946 Pooideae. *Plant Physiology*, 180 (1), 404-419.
- 947 Shafer, A. B., & Wolf, J. B. (2013). Widespread evidence for incipient ecological speciation: a
948 meta-analysis of isolation-by-ecology. *Ecology Letters*, 16 (7), 940-950.

- 949 Sommer, S., McDevitt, A. D., & Balkenhol, N. (2013). Landscape genetic approaches in
950 conservation biology and management. *Conservation Genetics*, 14 (2), 249-251.
- 951 Soreng, R. J., Peterson, P. M., Romaschenko, K., Davidse, G., Zuloaga, F. O., Judziewicz, E. J.,
952 ... & Morrone, O. (2015). A worldwide phylogenetic classification of the Poaceae
953 (Gramineae). *Journal of Systematics and Evolution*, 53 (2), 117-137.
- 954 Soreng, R. J., Peterson, P. M., Romaschenko, K., Davidse, G., Teisher, J. K., Clark, L. G., ... &
955 Zuloaga, F. O. (2017). A worldwide phylogenetic classification of the Poaceae
956 (Gramineae) II: An update and a comparison of two 2015 classifications. *Journal of*
957 *Systematics and Evolution*, 55 (4), 259-290.
- 958 Sork, V. L., Nason, J., Campbell, D. R., & Fernandez, J. F. (1999). Landscape approaches to
959 historical and contemporary gene flow in plants. *Trends in Ecology & Evolution*, 14 (6),
960 219-224.
- 961 Stange, M., Barrett, R. D., & Hendry, A. P. (2021). The importance of genomic variation for
962 biodiversity, ecosystems and people. *Nature Reviews Genetics*, 22 (2), 89-105.
- 963 St. Clair, B. J., Kilkenny, F. F., Johnson, R. C., Shaw, N. L., & Weaver, G. (2013). Genetic
964 variation in adaptive traits and seed transfer zones for *Pseudoroegneria spicata* (bluebunch
965 wheatgrass) in the northwestern United States. *Evolutionary Applications*, 6 (6), 933-948.
- 966 St. Clair, A. B., Dunwiddie, P. W., Fant, J. B., Kaye, T. N., & Kramer, A. T. (2020). Mixing source
967 populations increases genetic diversity of restored rare plant populations. *Restoration*
968 *Ecology*, 28 (3), 583-593.
- 969 Storfer, A., Murphy, M. A., Spear, S. F., Holderegger, R., & Waits, L. P. (2010). Landscape
970 genetics: where are we now?. *Molecular Ecology*, 19 (17), 3496-3514.

- 971 Stritt, C., Gimmi, E. L., Wyler, M., Bakali, A. H., Skalska, A., Hasterok, R., ... & Roulin, A. C.
972 (2022). Migration without interbreeding: evolutionary history of a highly selfing
973 Mediterranean grass inferred from whole genomes. *Molecular Ecology*, 31 (1), 70-85.
974 Svejcar, T., Boyd, C., Davies, K., Hamerlynck, E., & Svejcar, L. (2017). Challenges and
975 limitations to native species restoration in the Great Basin, USA. *Plant Ecology*, 218 (1),
976 81-94.
977 Tajima, F. (1989). Statistical method for testing the neutral mutation hypothesis by DNA
978 polymorphism. *Genetics*, 123 (3), 585-595.
979 Tchakerian, V. P., & Lancaster, N. (2002). Late Quaternary arid/humid cycles in the Mojave
980 senDesert and western Great Basin of North America. *Quaternary Science Reviews*, 21 (7),
981 799-810.
982 Team, R. C. (2013). R: A language and environment for statistical computing.
983 Templeton, A. R. (1986). Coadaptation and outbreeding depression. *Conservation biology: the*
984 *science of scarcity and diversity*, 105-116.
985 Verdú, M., Gómez-Aparicio, L., & Valiente-Banuet, A. (2012). Phylogenetic relatedness as a tool
986 in restoration ecology: a meta-analysis. *Proceedings of the Royal Society B: Biological*
987 *Sciences*, 279 (1734), 1761-1767.
988 Vogel, J. P., Tuna, M., Budak, H., Huo, N., Gu, Y. Q., & Steinwand, M. A. (2009). Development
989 of SSR markers and analysis of diversity in Turkish populations of *Brachypodium*
990 *distachyon*. *BMC Plant Biology*, 9 (1), 1-11.
991 Volis, S., Zaretsky, M., & Shulgina, I. (2010). Fine-scale spatial genetic structure in a
992 predominantly selfing plant: role of seed and pollen dispersal. *Heredity*, 105 (4), 384-393.

- 993 Wagner, V., Durka, W., & Hensen, I. (2011). Increased genetic differentiation but no reduced
994 genetic diversity in peripheral vs. central populations of a steppe grass. *American Journal
995 of Botany*, 98 (7), 1173-1179.
- 996 Wagner, V., Treiber, J., Danihelka, J., Ruprecht, E., Wesche, K., & Hensen, I. (2012). Declining
997 genetic diversity and increasing genetic isolation toward the range periphery of *Stipa*
998 *pennata*, a Eurasian feather grass. *International Journal of Plant Sciences*, 173 (7), 802-
999 811.
- 1000 Wang, I. J., Glor, R. E., & Losos, J. B. (2013). Quantifying the roles of ecology and geography in
1001 spatial genetic divergence. *Ecology Letters*, 16 (2), 175-182.
- 1002 Wang, I. J., & Bradburd, G. S. (2014). Isolation by environment. *Molecular Ecology*, 23 (23),
1003 5649-5662.
- 1004 West, N. E. (1983). Great Basin-Colorado plateau sagebrush semi-desert. *Temperate Deserts and
1005 Semi-deserts*, 5, 331-369.
- 1006 Williams, C. F., Ruvinsky, J., Scott, P. E., & Hews, D. K. (2001). Pollination, breeding system,
1007 and genetic structure in two sympatric *Delphinium* (Ranunculaceae) species. *American
1008 Journal of Botany*, 88 (9), 1623-1633.
- 1009 Wright, S. (1943). Isolation by distance. *Genetics*, 28 (2), 114.
- 1010 Xu, S., Wang, J., Guo, Z., He, Z., & Shi, S. (2020). Genomic convergence in the adaptation to
1011 extreme environments. *Plant Communications*, 1 (6), 100117.
- 1012

1013 **Tables**

1014 **Table 1.** Population genetic summary statistics for each sampled *A. thurberianum* population. For
1015 each sampling location (population), the table shows the number of individuals (N), expected (H_e)
1016 and observed heterozygosity (H_o), inbreeding coefficient (F_{IS}), nucleotide diversity (π), Tajima's
1017 D (D), standardized index of association (r^-_d), and index of association (I_A). Significant F_{IS} results
1018 based on bootstrap coefficient intervals are depicted with an asterisk. The seed zone for each
1019 population corresponds to those proposed by Johnson et al., (2017). The MD population has no
1020 seed zone information as it was located outside of the Johnson et al., (2017) projected area.

1021

| Population name, Population | State | abbr. | N | H_e | H_o | F_{IS} | π | D | r^-_d | I_A | Seed zone |
|-----------------------------|-------|-------|----|-------|-------|----------|-------|-------|---------|---------|-----------|
| Austin Hwy, NV | AH | AH | 14 | 0.029 | 0.007 | 0.719* | 0.039 | 0.487 | 0.283 | 122.350 | 8 |
| Austin Summit, NV | AS | AS | 15 | 0.028 | 0.010 | 0.649* | 0.027 | 0.519 | 0.226 | 93.120 | 5 |
| Bald Mountain, NV | BM | BM | 18 | 0.025 | 0.008 | 0.671* | 0.025 | 1.030 | 0.186 | 58.549 | 4 |
| Buena Vista, OR | BV | BV | 15 | 0.066 | 0.029 | 0.509* | 0.067 | 0.339 | 0.019 | 21.443 | 8 |
| Dayton Hill, NV | DH | DH | 14 | 0.044 | 0.011 | 0.728 | 0.045 | 0.577 | 0.137 | 87.699 | 8 |
| East Walker, CA | EW | EW | 15 | 0.028 | 0.011 | 0.704 | 0.028 | 0.307 | 0.314 | 148.414 | 11 |
| Finger Rock, NV | FR | FR | 14 | 0.026 | 0.010 | 0.675* | 0.026 | 0.487 | 0.271 | 106.050 | 7 |
| Grey's Butte, NV | GB | GB | 14 | 0.060 | 0.024 | 0.522* | 0.061 | 0.311 | 0.090 | 89.900 | 5 |
| Hwy 140, NV | HO | HO | 15 | 0.052 | 0.024 | 0.484* | 0.052 | 0.252 | 0.025 | 22.540 | 8 |
| Jones Canyon, NV | JC | JC | 15 | 0.059 | 0.014 | 0.740* | 0.058 | 0.752 | 0.102 | 86.020 | 11 |
| Long Valley, CA | LV | LV | 14 | 0.075 | 0.012 | 0.816* | 0.074 | 0.512 | 0.236 | 270.389 | 8 |
| Modoc, CA | MD | MD | 15 | 0.058 | 0.016 | 0.715* | 0.057 | 0.483 | 0.047 | 43.020 | NA |
| Peavine Low, NV | PL | PL | 15 | 0.049 | 0.032 | 0.368* | 0.054 | 0.787 | 0.180 | 121.440 | 5 |
| Patagonia, NV | PT | PT | 12 | 0.035 | 0.024 | 0.344* | 0.041 | 0.183 | 0.133 | 81.633 | 5 |
| Smith Creek, NV | SC | SC | 15 | 0.030 | 0.010 | 0.611 | 0.029 | 0.536 | 0.329 | 143.590 | 8 |
| Spanish Springs, CA | SS | SS | 14 | 0.060 | 0.024 | 0.551 | 0.067 | 0.273 | 0.029 | 29.786 | 5 |
| Virginia Mountains, NV | VM | VM | 12 | 0.049 | 0.017 | 0.603 | 0.054 | 0.401 | 0.084 | 64.681 | 8 |

1022 **Table 2.** ANOVA results showing the variance explained by each environmental variable in the
1023 partial RDA, the *F* value, and the associated *p* value.

1024

| Environmental Variables | Description | df | Variance | F | p |
|-------------------------|---|-----|----------|--------|--------|
| MaxCWD | Magnitude of climatic water deficit | 1 | 21.001 | 28.743 | 0.0009 |
| AfRad | Folded aspect converted to radians | 1 | 17.772 | 24.323 | 0.0009 |
| prcpsum | PRISM total precipitation from June-Aug | 1 | 16.801 | 22.994 | 0.0009 |
| WsAETspr | Difference between water supply and AET during the spring | 1 | 15.934 | 21.807 | 0.0009 |
| mxtmpwin | PRISM average max temp from Dec-Feb (C°) | 1 | 15.715 | 21.507 | 0.0009 |
| FallAET | Difference between actual evapotranspiration summer low and fall peak | 1 | 14.417 | 19.731 | 0.0009 |
| SlopRad | Slope converted to radians | 1 | 13.412 | 18.356 | 0.0009 |
| AETgdd | Cumulative annual actual evapotranspiration during the growing season | 1 | 11.450 | 15.671 | 0.0009 |
| | Residuals | 233 | 170.245 | | |

1025

1026

1027

1028

1029

1030

1031

1032

1033 **Table 3.** Molecular analysis of variance (AMOVA) results for the 17 populations of *Achnatherum*
1034 *thurberianum*. Here, we provide the degrees of freedom (df), sum of squares (SS), mean squares
1035 (MS), total variance (sigma), and the percentage of variance explained by each source of variation
1036 (Variance %).

1037

| Source of variation | df | SS | MS | Sigma | Variance % |
|----------------------------|-----------|-----------|-----------|--------------|-------------------|
| Between populations | 16 | 203377.59 | 12711.09 | 863.60 | 79.66 |
| Within populations | 229 | 50468.42 | 220.38 | 220.38 | 20.33 |
| Total | 245 | 253846.01 | 1036.10 | 1083.99 | 100 |

1038

1039

1040 **Table 4.** The influence of climate, structure, and geography on genetic variation decomposed with
1041 partial RDA. The proportion of explainable variance represents the total constrained variation
1042 explained by the full model.

1043

| Partial RDA models | Variance | R ² | p value | Proportion of explainable Variance | Proportion of total Variance |
|--|----------|----------------|---------|------------------------------------|------------------------------|
| Full model: $F \sim \text{clim.} + \text{geog.} + \text{struct.}$ | 276.21 | 0.59 | 0.001 | 1 | 0.59 |
| Pure climate: $F \sim \text{clim.} (\text{geog.} + \text{struct.})$ | 110.23 | 0.23 | 0.001 | 0.39 | 0.23 |
| Pure structure: $F \sim \text{struct.} (\text{clim.} + \text{geog.})$ | 49.93 | 0.10 | 0.001 | 0.17 | 0.10 |
| Pure geography: $F \sim \text{geog.} (\text{clim.} + \text{struct.})$ | 19.53 | 0.04 | 0.001 | 0.06 | 0.03 |
| Confounded climate/structure/geography | 96.52 | | | 0.33 | 0.19 |
| Total unexplained | 189.92 | | | | |
| Total variance | 466.13 | | | | |

1044

1045

1046

1047

1048

1049

1050

1051

1052

1053

1054 **Figure Legends**

1055

1056 **Figure 1.** Population genetic structure of 17 populations of *Achnatherum thurberianum* based on
1057 5,677 SNPs. a) Map of the sampled locations with each population code. Each population is
1058 colored consistently in panels a, b, and c, and represented by one of five shapes corresponding to
1059 the seed zone of Johnson et al. (2017) containing each population (Table 1). b) The first and second
1060 principal components (PCs) resulting from PCA on the genotypic data plotted for each individual.
1061 c) Each individual plotted for the first two axes from a Uniform Manifold Approximation and
1062 Projection (UMAP) clustering analysis based on the genotypic data. d) ADMIXTURE plot
1063 representing estimated ancestry coefficients for each individual, following results of an analysis
1064 with K set to eight ancestral populations.

1065

1066 **Figure 2.** Mantel test results and relationships between genetic (Nei's D) and geographic distances
1067 (km) (a), genetic (Nei's D) and environmental distances (b), and geographic (km) and
1068 environmental distances (c).

1069

1070 **Figure 3.** Landscape genetic differentiation for the 17 *Achnatherum thurberianum* populations. a)
1071 Map of the sampled locations with each population (colors) and seed zone (symbols) code (Table
1072 1). b) Estimated effective migration surface (EEMS) plot depicting estimated migration rates (in
1073 log 10 scale) that deviate from isolation by distance expectations. Brown represents areas of low
1074 effective migration relative to the average, and green represents areas of higher effective migration.
1075 c) Unbundled principal components (unPC) representation; higher unPC values, representing
1076 greater differentiation than expected among populations, are colored in progressively darker

1077 shades of brown, while lower unPC values, representing lower differentiation among populations,
1078 are colored in progressively darker shades of green. The unPC values near the mean of the
1079 distribution are colored in white.

1080

1081 **Figure 4.** Population phylogenetic differentiation of the 17 *Achnatherum thurberianum*
1082 populations. a) Maximum likelihood topology inferred with IQ-TREE. The scale bar represents the
1083 expected number of nucleotide substitutions per site. Ultrafast bootstrap support values (UFBS)
1084 are indicated at the nodes. b) Projected phylogeny onto the geographic map showing each
1085 population's location. One individual is represented for each population to minimize overlap. The
1086 different symbols in both panels correspond to the different seed zones studied (Table 1).

1087

1088 **Figure 5.** Redundancy analysis (RDA) plot depicting the environmental variables studied
1089 significantly associated with genetic variation. The direction and length of arrows correspond to
1090 the loadings of each variable on the two RDA axes.

Figure 1.

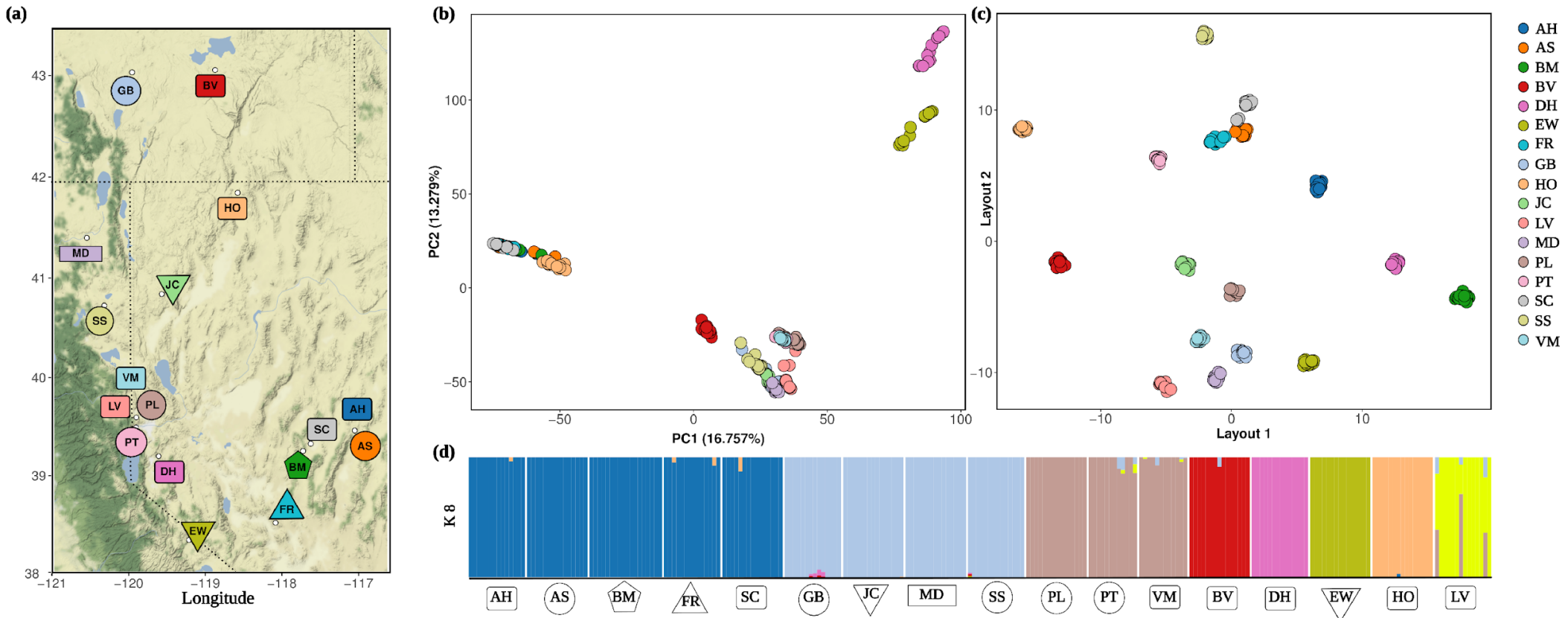


Figure 2.

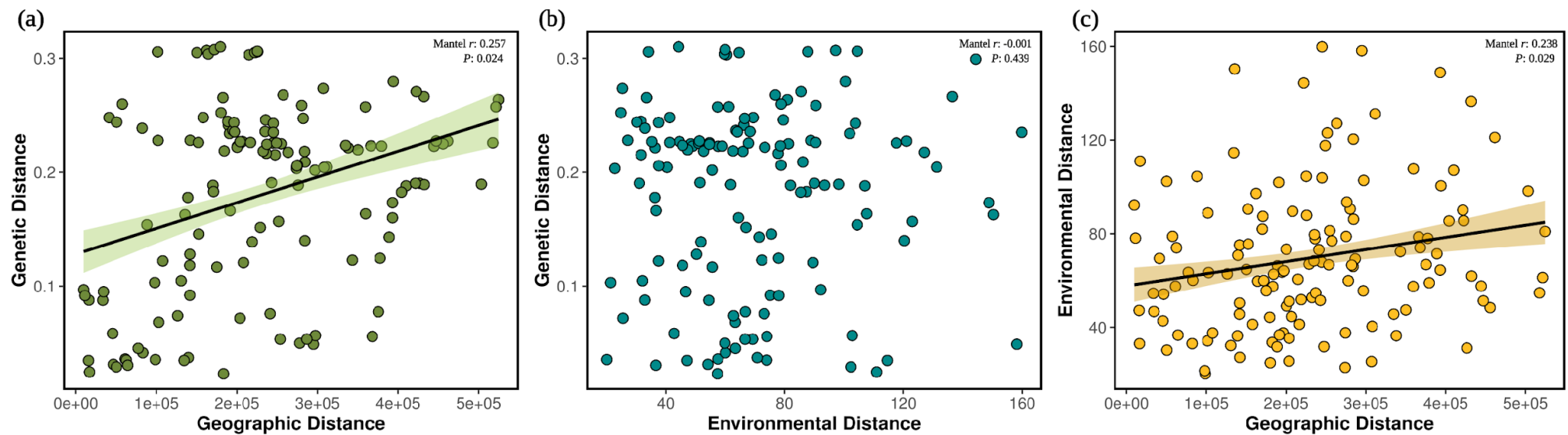


Figure 3.

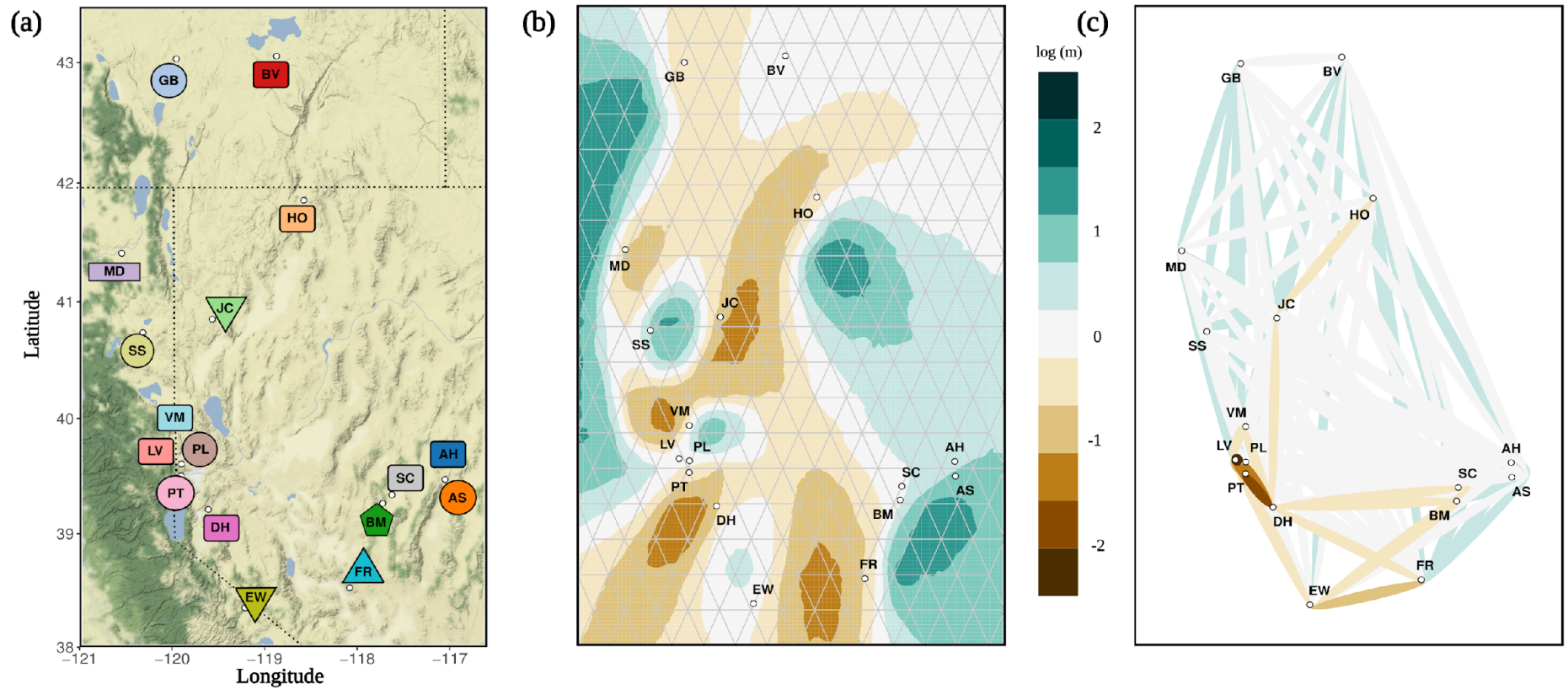


Figure 4.

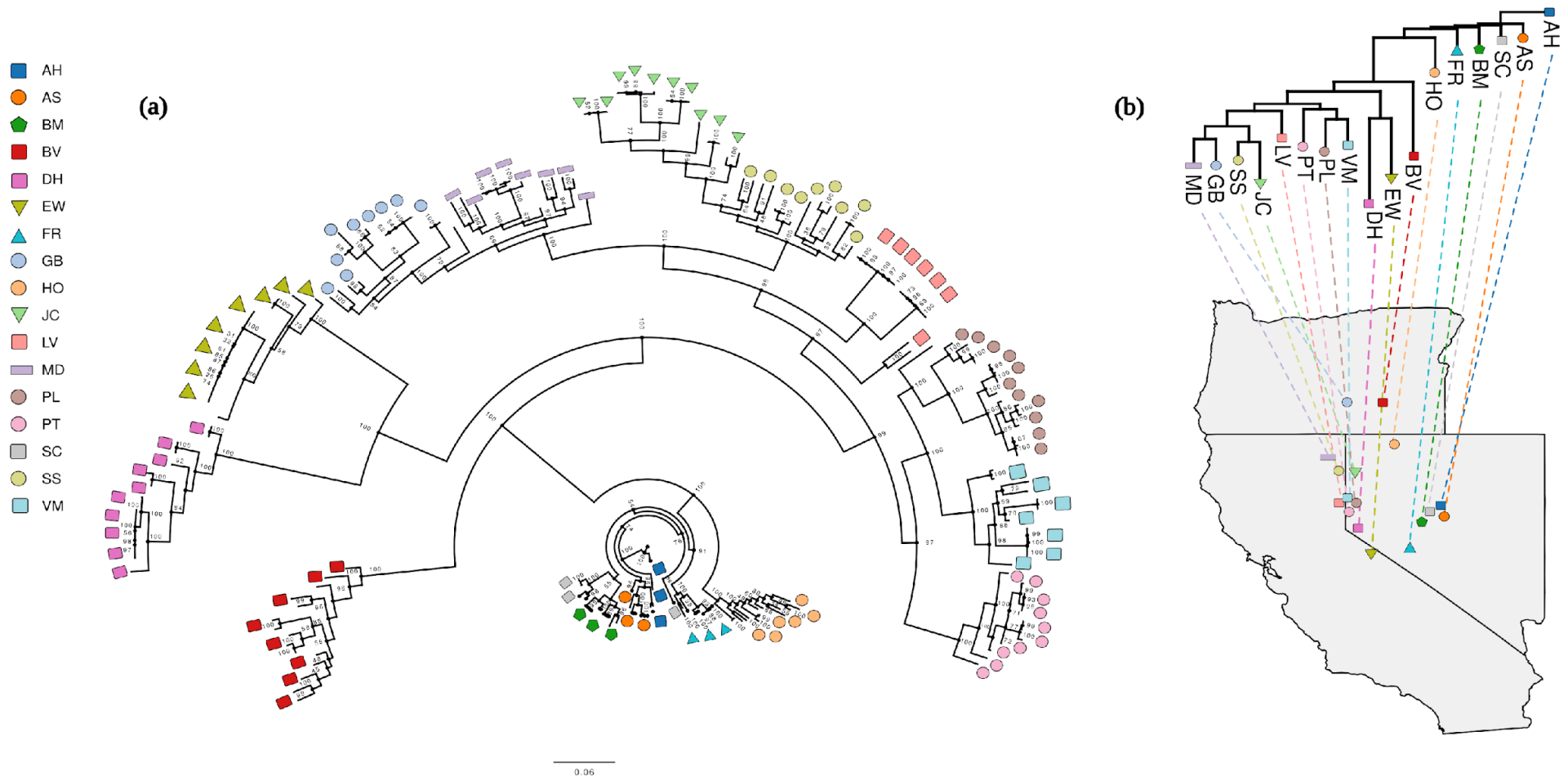


Figure 5.

